World Journal of Gastroenterology

Submit a Manuscript: https://www.f6publishing.com

World J Gastroenterol 2022 July 28; 28(28): 3644-3665

DOI: 10.3748/wjg.v28.i28.3644

ISSN 1007-9327 (print) ISSN 2219-2840 (online)

ORIGINAL ARTICLE

Basic Study

Mechanism of electroacupuncture and herb-partitioned moxibustion on ulcerative colitis animal model: A study based on proteomics

Qin Qi, Rui Zhong, Ya-Nan Liu, Chen Zhao, Yan Huang, Yuan Lu, Zhe Ma, Han-Dan Zheng, Lu-Yi Wu

Specialty type: Gastroenterology and hepatology

Provenance and peer review: Unsolicited article; Externally peer reviewed.

Peer-review model: Single blind

Peer-review report's scientific quality classification

Grade A (Excellent): A
Grade B (Very good): 0
Grade C (Good): C, C
Grade D (Fair): 0
Grade E (Poor): 0

P-Reviewer: Moldogazieva NT, Russia; Saleem S, Pakistan

Received: September 3, 2021
Peer-review started: September 3, 2021
First decision: November 7, 2021
Revised: November 19, 2021
Accepted: June 24, 2022
Article in press: June 24, 2022
Published online: July 28, 2022

Qin Qi, Ya-Nan Liu, Yan Huang, Yuan Lu, Zhe Ma, Han-Dan Zheng, Lu-Yi Wu, Yueyang Hospital of Integrated Traditional Chinese and Western Medicine, Shanghai University of Traditional Chinese Medicine, Shanghai 200437, China

Rui Zhong, Shanghai QiGong Research Institute, Shanghai University of Traditional Chinese Medicine, Shanghai 200030, China

Chen Zhao, School of Acupuncture, Moxibustion and Tuina, Shanghai University of Traditional Chinese Medicine, Shanghai 201203, China

Corresponding author: Lu-Yi Wu, PhD, Associate Professor, Yueyang Hospital of Integrated Traditional Chinese and Western Medicine, Shanghai University of Traditional Chinese Medicine, No. 110 Ganhe Road, Hongkou District, Shanghai 200437, China.
luyitcm@163.com

Abstract

BACKGROUND

Ulcerative colitis (UC) is a chronic, nonspecific intestinal inflammatory disease. Acupuncture and moxibustion is proved effective in treating UC, but the mechanism has not been clarified. Proteomic technology has revealed a variety of biological markers related to immunity and inflammation in UC, which provide new insights and directions for the study of mechanism of acupuncture and moxibustion treatment of UC.

AIM

To investigate the mechanism of electroacupuncture (EA) and herb-partitioned moxibustion (HM) on UC rats by using proteomics technology.

METHODS

Male Sprague-Dawley rats were randomly divided into the normal (N) group, the dextran sulfate sodium (DSS)-induced UC model (M) group, the HM group, and the EA group. UC rat model was prepared with 3% DSS, and HM and EA interventions at the bilateral Tianshu and Qihai acupoints were performed in HM or EA group. Haematoxylin and eosin staining was used for morphological evaluation of colon tissues. Isotope-labeled relative and absolute quantification (iTRAQ) and liquid chromatography-tandem mass spectrometry were performed for proteome analysis of the colon tissues, followed by bioinformatics analysis and protein-protein interaction networks establishment of differentially expressed

proteins (DEPs) between groups. Then western blot was used for verification of selected DEPs.

RESULTS

The macroscopic colon injury scores and histopathology scores in the HM and EA groups were significantly decreased compared to the rats in the M group ($P < 0.01$). Compared with the N group, a total of 202 DEPs were identified in the M group, including 111 up-regulated proteins and 91 down-regulated proteins, of which 25 and 15 proteins were reversed after HM and EA interventions, respectively. The DEPs were involved in various biological processes such as biological regulation, immune system progression and in multiple pathways including natural killer cell mediated cytotoxicity, intestinal immune network for immunoglobulin A (IgA) production, and FcγR-mediated phagocytosis. The Kyoto Encyclopedia of Genes and Genomes pathways of DEPs between HM and M groups, EA and M groups both included immune-associated and oxidative phosphorylation. Network analysis revealed that multiple pathways for the DEPs of each group were involved in protein-protein interactions, and the expression of oxidative phosphorylation pathway-related proteins, including ATP synthase subunit g (ATP5L), ATP synthase beta subunit precursor (Atp5f), cytochrome c oxidase subunit 4 isoform 1 (Cox4i1) were down-regulated after HM and EA interventions. Subsequent verification of selected DEPs (Synaptic vesicle glycoprotein 2A; nuclear cap binding protein subunit 1; carbamoyl phosphate synthetase 1; Cox4i1; ATP synthase subunit b, Atp5f1; doublecortin like kinase 3) by western blot confirmed the reliability of the iTRAQ data, HM and EA interventions can significantly down-regulate the expression of oxidative phosphorylation-associated proteins (Cox4i1, Atp5f1) ($P < 0.01$).

CONCLUSION

EA and HM could regulate the expression of ATP5L, Atp5f1, Cox4i1 that associated with oxidative phosphorylation, then might regulate immune-related pathways of intestinal immune network for IgA production, FcγR-mediated phagocytosis, thereby alleviating colonic inflammation of DSS-induced UC rats.

Key Words: Proteomics; Ulcerative colitis; Moxibustion; Electroacupuncture; Differential proteins

Core Tip: Ulcerative colitis (UC) is a nonspecific inflammatory bowel disease with unclear etiology. Acupuncture and moxibustion are benefit to UC by improving colonic mucosa damage, regulating inflammatory cytokines. In recent years, proteomic technology has been widely used in the study of UC, revealing a variety of biological markers related to immunity and inflammation in UC. We applied isotope-labeled relative and absolute quantification proteomics technology to identify UC-relevant protein targets and further explore the mechanism of acupuncture and moxibustion. It was found that electroacupuncture and herb-partitioned moxibustion could regulate the expression of multiple proteins, such as ATP synthase subunit g, ATP synthase beta subunit precursor 1, cytochrome c oxidase subunit 4 isoform 1 that associated with oxidative phosphorylation, that might regulate immune-related pathways, thereby alleviating colonic inflammation of dextran sulfate sodium-induced UC rats.

Citation: Qi Q, Zhong R, Liu YN, Zhao C, Huang Y, Lu Y, Ma Z, Zheng HD, Wu LY. Mechanism of electroacupuncture and herb-partitioned moxibustion on ulcerative colitis animal model: A study based on proteomics. *World J Gastroenterol* 2022; 28(28): 3644-3665
URL: https://www.wjgnet.com/1007-9327/full/v28/i28/3644.htm
DOI: https://dx.doi.org/10.3748/wjg.v28.i28.3644

INTRODUCTION

Ulcerative colitis (UC) is a chronic, nonspecific inflammatory disease, with lesions are mainly confined to the large intestinal mucosa and submucosal layer. Mucosal inflammation at the affected site is characterized by a diffuse distribution and its clinical manifestations mainly include abdominal pain, diarrhoea, mucus pus and blood in stool[1]. UC has a prolonged disease course, which can lead to the development of colorectal cancer, accounting for 10% to 15% of deaths among patients with UC, and is listed as one of the refractory diseases by the World Health Organization. Epidemiological data show that the prevalence of UC in Asia has increased exponentially in recent years, and the growth rate of UC

in some East Asian countries including China has increased in multiples over the past decade[2,3].

The pathogenesis of UC is not yet clear, but it is believed to be related to genetic susceptibility, epithelial barrier deficiency, immune disorders, and environmental factors[4]. The modern treatment methods for UC mainly include glucocorticoids, immunosuppressants, 5-aminosalicylic acid, and biological agents (monoclonal antibodies), but it is prone to relapse after drug withdrawal, and multiple drugs have adverse side effects. Therefore, active exploration of the pathogenesis of UC, identification of disease biomarkers, and screening of specific therapeutic targets are important for the diagnosis and treatment of UC. As one of the unique treatments of traditional Chinese medicine, acupuncture and moxibustion have significant efficacy and advantages in the treatment of UC[5-7], but the specific mechanism requires further clarification.

In recent years, proteomic technology has been widely used in the study of UC[8,9], revealing a variety of biological markers related to immunity and inflammation in UC[10]. The activity of mitochondrial oxidative phosphorylation complex in intestinal tissues of UC patients decreases, and the dysfunction of mitochondrial oxidative phosphorylation may be involved in the pathogenesis of UC, but it is not clear whether acupuncture and moxibustion have a regulatory effect on it. Therefore, our study used isotope-labeled relative and absolute quantification (iTRAQ) proteomics technology to quantitatively analyse proteins in the colon tissues of UC rats, to analyse the biological functions of differentially expressed proteins (DEPs) and observe changes of immune and oxidative phosphorylation-associated protein expression profiles in colon tissues of UC rats and regulatory effect of acupuncture and moxibustion, in order to identify UC-relevant protein targets and further explore the mechanism of effects of acupuncture and moxibustion on UC.

MATERIALS AND METHODS

Animals

Healthy clean grade naïve male Sprague-Dawley (SD) rats, aged 6 wk, with body weight of 180 ± 20 g were purchased from Shanghai Slac Laboratory Animal Co., Ltd. [Laboratory Animal Use Permit No. SYXK (Shanghai) 2014-0008] and housed in the Experimental Animal Center of Shanghai University of Traditional Chinese Medicine. The animal protocol was designed to minimize pain or discomfort to the animals. The housing environment was a 12 h circadian rhythm, with a room temperature of 20 ± 2 °C and 50%-70% indoor humidity, 4 rats per cage, and rats were free to standard food and pure water. This study was approved by the Ethics Committee of the Experimental Animal Center of Shanghai University of Traditional Chinese Medicine. We tried all efforts to minimize animal suffering.

Dextran sulfate sodium-induced UC model preparation

For preparing the UC rat model, the rats received 3% dextran sulfate sodium (DSS, molecular weight: 36000-50000, MP Biomedicals, United States) in drinking water by oral for 7 d, and then were switched to pure water for 7 d, and the same procedures were repeated once (drinking 3% DSS solution for 7 d, followed by drinking pure water for 7 d)[11]. After modeling, rats were anaesthetized *via* intraperitoneal injection with 2% pentobarbital sodium (30-40 mg/kg) (P3761, Sigma, United States) for tissue collection, the gross injury and hematoxylin and eosin (HE) staining were used to evaluate whether the model was successfully established.

Grouping and interventions

After one week of adaptive feeding, 32 rats were randomly divided into the normal (N) group, the DSS-induced UC model (M) group, the herb-partitioned moxibustion (HM) group, and the electroacupuncture (EA) group, with 8 rats in each group. UC rat model was prepared by DSS except for the N group. After model establishment, the rats in the HM and EA group were treated with corresponding treatment at Tianshu (ST25, bilateral) and Qihai (CV6) acupoints[12]. In the HM group, Chinese medicine powder containing Coptis chinensis, Radix aconiti lateralis, Cortex Cinnamomi, Radix aucklandiae, Flos carthami, Salvia miltiorrhiza, and Angelica sinensis was mixed and stirred with yellow wine to make herbal cake, then an herbal cake was prepared with a thickness of 0.5 cm and a diameter of 1 cm using a specific mould, and conical moxa cones weighing approximately 90 mg were made with moxa (Nanyang Hanyi Moxa Co., Ltd., Nanyang, China) by a mould. The rats were supine immobilized on a self-made fixator, the prepared moxa cone was placed on the top of herbal cake, and the herbal cake was placed at the ST25 and CV6 acupoints, then the moxa cone was ignited using line incense, 2 moxa cones per acupoint per time, once a day for 7 d (Figure 1)[13]. In the EA group, the rats were also supine immobilized on the self-made fixator, a 0.25 mm × 25 mm acupuncture needle was inserted into the ST25 and CV6 acupoints for 5 mm, then the needle handle was connected to a Han's-200 acupoint nerve stimulator, with a frequency of 2/100 Hz and a current of 1 mA. The needle was kept for 10 min per time, once a day for a total of 7 d[14]. The rats in the N group and the M group did not receive any treatment, but only the same grasping fixation as that in the treatment groups at 10 o'clock every day for a total of 7 d.

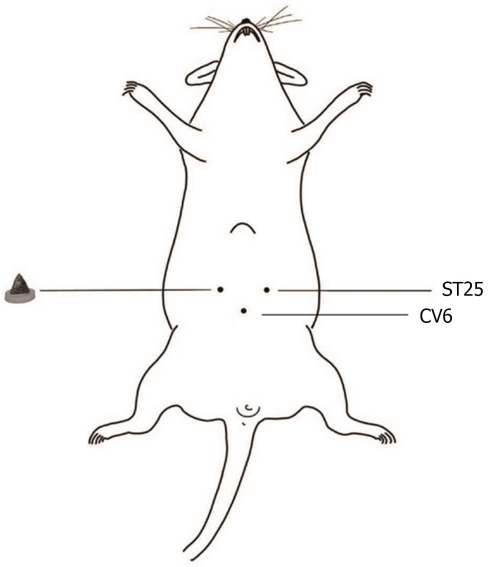

Figure 1 Schematic diagram of herb-partitioned moxibustion at the rat Tianshu (ST25, bilateral) and Qihai (CV6) acupoints.

Collection of colon tissue and macroscopic scoring of colon injury

After the intervention, rats were anaesthetized with intraperitoneal injection of 2% pentobarbital sodium. The abdominal cavity was exposed and the entire colon from the pubic symphysis to the distal cecum was collected, and the length of the colon was recorded. The distal colon with a length of 6-8 cm was collected and cut longitudinally along the mesentery, observed the gross morphology, the macroscopic scoring of the colon was performed according to the following parameters: Hyperemia, wall thickening, ulceration, inflammation extension, and damage no damage, score 0; hyperemia without ulcers, score 1; hyperemia and wall thickening without ulcers, score 2; one ulceration site without wall thickening, score 3; two or more ulceration sites, score 4; 0.5 cm extension of inflammation or major damage, score 5; 1 cm extension of inflammation or severe damage, score 6[15]. Then was cut into two parts transversely, one part was fixed in 4% paraformaldehyde for morphological observation, and the remaining part was placed in liquid nitrogen for 1 h and transferred to a -80 °C freezer for future detection.

Morphological observation of the colon

Colon tissues fixed in 4% paraformaldehyde fixative solution were dehydrated, embedded in paraffin, and sliced into 4 μm sections for HE staining with the following steps: Dewaxing in xylene I and II solutions for 20 min each; elution in 100%, 95%, 90%, 80%, and 70% ethanol for 5 min each; rinsing with double distilled water for 5 min × 2 times; haematoxylin staining for 2-3 min; rinsing with running water for 10 min; 1% hydrochloric acid ethanol differentiation solution for 1-2 s; rinsing with running water for 5 min; eosin dye staining for 2-3 min; dehydration in 70%, 80%, 90%, and 100% ethanol for 1-2 s each; xylene I and II solutions for 15 min each. After drying and sealing, the colon sections were observed under a light microscope and microscopic scoring of the colon was performed according to the following parameters: Damage/necrosis, inflammatory cell infiltration, submucosal edema, and hemorrhage of mucosa. Colonic gross damage scores were recorded according to the severity of changes: No change, score 0; mild, score 1; moderate, score 2; severe, score 3[16].

Proteomic analysis

Protein extraction and enzymatic digestion: Colon samples from 3 rats in each group were randomly collected and ground into powder, and an appropriate amount of radioimmunoprecipitation assay (RIPA) protein lysis buffer (R0010, Solarbio, United States) was added (150 μL RIPA was add to 20 mg colon tissue), high-abundance protein in the sample was removed, a 5-fold volume of 10% trichloroacetic acid/cold acetone was added to the sample and precipitated at -20 °C overnight. The precipitated proteins were centrifuged at 4 °C, 15000 g for 20 min, the supernatant was removed, and samples were air-dried and precipitated after repeating the above steps several times. After lysis, samples were centrifuged at 25000 g for 20 min at 4 °C, and the supernatant was the protein solution. A total of 100 μg of protein solution was collected from each sample, and trypsin (2.5 μg) was added to the protein solution at a ratio of 40: 1 of protein: Enzyme, enzymolysis at 37 °C for 4 h. Trypsin was then added according to the above ratio and continue enzymolysis at 37 °C for 8 h.

Peptide labelling and separation: The digested peptide fragments were desalted using a Strata X column and vacuum-dried. The peptide samples were dissolved in 0.5 M triethylammonium

bicarbonate, and then were were labeled with iTRAQ (iTRAQ8-plexreagent kit, Sigma, United States) and maintained at room temperature for 2 h. The Shimadzu LC-20AB liquid chromatography system (separation column: 5 μm, 4.6 mm × 250 mm Gemini C18) was used for liquid phase separation of samples. Dried peptide samples were redissolved in 2 mL of mobile phase A (5% ACN, pH 9.8), the solution was loaded, and gradient elution was performed at a flow rate of 1 mL/min as follows: 5% mobile phase B (95% ACN, pH 9.8) for 10 min, 5%-35% mobile phase B for 40 min, 35%-95% mobile phase B for 1 min, mobile phase B for 3 min, and equilibration with 5% mobile phase B for 10 min. The elution peak was monitored at a wavelength of 214 nm, and 1 fractionated peptide was collected every minute. The chromatographic elution peaks were combined with the samples to obtain 20 fractionated peptides, which were then freeze-dried.

High-performance liquid chromatography: The dried peptide samples were redissolved using mobile phase A (2% ACN, 0.1% FA) and centrifuged at 20000 g for 10 min. The supernatant was collected and loaded onto the column, and samples were separated by a Prominence nano LC (LC-20AD, Shimadzu, Japan). The sample was first enriched in a trap column and desalted, and the tandem self-assembled C18 column (75-μm inner diameter, 3.6-μm pore size, 15-cm length) was used. Separation was performed at a flow rate of 300 nL/min through an effective gradient: at 0-8 min, 5% mobile phase B (98% ACN, 0.1% FA); at 8-43 min, mobile phase B increased linearly from 8% to 35%; at 43-48 min, mobile phase B increased from 35% to 60%; at 48-50 min, mobile phase B increased from 60% to 80%; at 50-55 min, 80% mobile phase B; and at 55-65 min, 5% mobile phase B.

Mass spectrometric detection: The separated peptides were transferred into an electrospray ionization tandem mass spectrometer: TripleTOF 5600 (SCIEX, Framingham, United States) and theion source was Nanospray III source (SCIEX, Framingham, United States). During data collection, the parameters of the mass spectrometer were set as follows: An ion source spray voltage of 2300 V, a nitrogen pressure of 30 psi, atomizer 15, and a spray interface temperature of 150 °C. High-sensitivity mode was used for scanning. The cumulative time of primary mass spectrometry scanning was 250 ms, and the cumulative of secondary mass spectrometry scanning time was 100 ms.

iTRAQ quantification and bioinformatics analysis

ITRAQ quantification was performed using IQuant software. The selection of significantly DEPs in a single experiment were as follows: Fold change (FC) ≥ 1.2 was set as up-regulation and FC ≤ 0.83 as down-regulation, as well as Q-value < 0.05. The Gene Ontology (GO) database was used for functional annotation analysis of DEPs. The Kyoto Encyclopedia of Genes and Genomes (KEGG) pathway database was used for pathway enrichment analysis of DEPs. The protein-protein interaction network was performed using STRING software with an interaction confidence of 0.7 (the maximum confidence was 1). Cytoscape (v.3.7.1) software was used to visualize the enrichment analysis results. Figure 2 showed the process of proteomics detection and analysis.

Western blot analysis

We selected DEPs in UC that were reversed by HM and EA for verification by using western blot method. Total proteins were extracted from colon tissues using RIPA buffer supplemented with protease and phosphatase inhibitors. Protein concentration was measured with the bicinchoninic acid protein concentration assay kit. The proteins were separated by polyacrylamide gelelectrophoresis method, with the voltage of concentrated glue was 90 V and that of separating glue was 120 V (BIO-RAD, 1645050), then the separated proteins were transferred to polyvinylidene fluoride membranes. The modified membranes were blocked with 5% bovine serum albumin in TBST, and then was incubated overnight at 4 °C with primary antibody. The antibody dilutions were prepared according to the instructions [Synaptic vesicle glycoprotein 2A (Sv2a), 1: 1000; nuclear cap binding protein subunit 1 (Ncbp1), 1: 800; Cps, 1: 5000; cytochrome c oxidase subunit 4 isoform 1 (Cox4i1), 1: 2000; ATP synthase beta subunit precursor 1 (Atp5f1), 1: 1000; doublecortin like kinase 3 (Dclk3), 1: 800)]. The membranes were washed with western detergent at room temperature for 6 times, 5 min each and then were incubated with secondary antibodies at room temperature for 1 h. Followed by washed with western detergent at room temperature for 6 times, 5 min each. The membranes were stained with enhanced chemiluminescence solution and visualized in a gel imager system (Tanon, 4600).

Statistical analysis

The western blot analysis data were analyzed with SPSS 20.0 statistical software. Data that consistent with the normal distribution were presented as mean ± SD, and one-way analysis of variance was used for comparison between groups, followed by the Fisher's Least significant difference method if data met the homogeneity of variance. For data that did not meet the normal distribution were presented as medians (P_{25}, P_{75}), and nonparametric test was used for comparison. $P < 0.05$ was considered statistically significance.

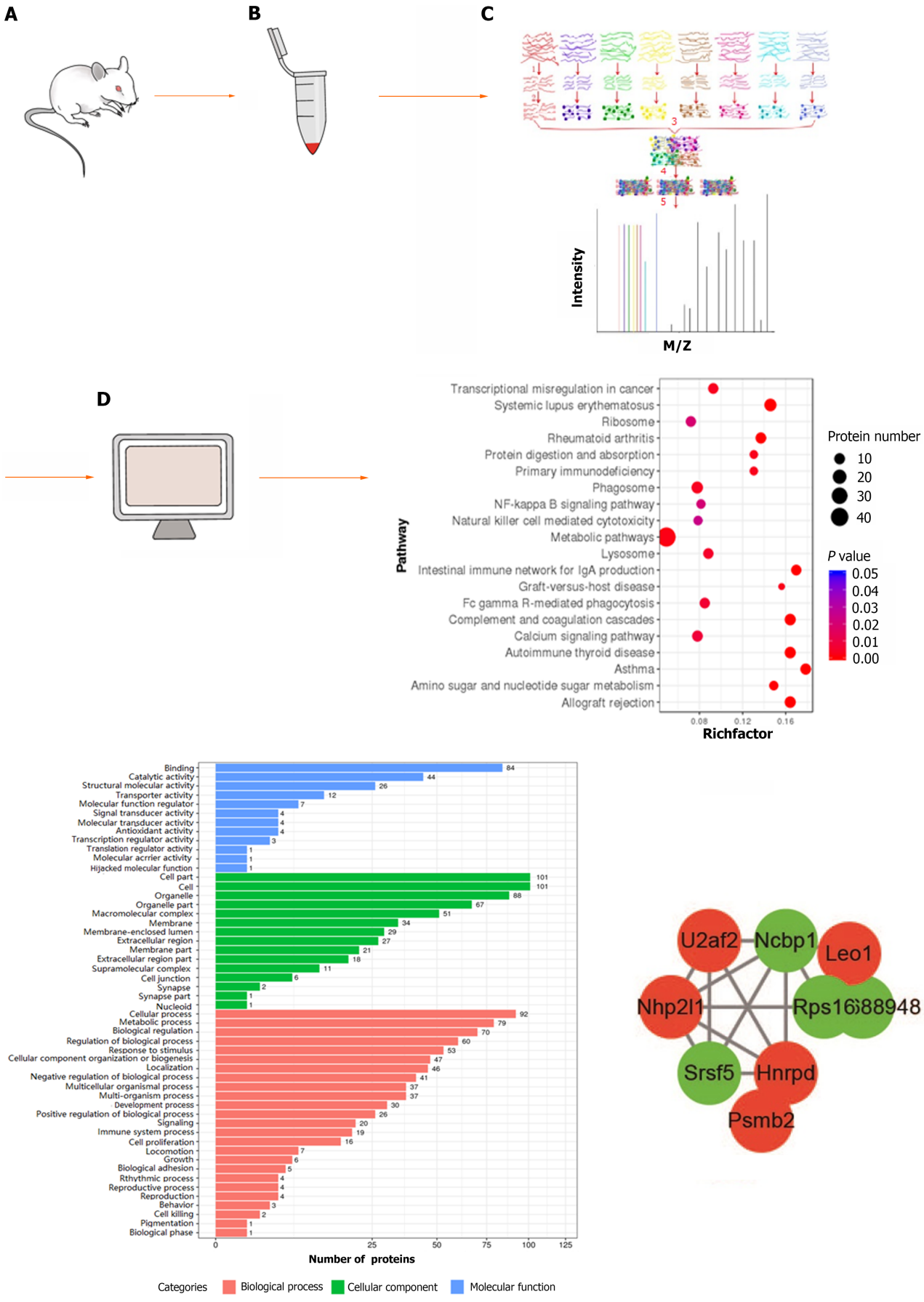

Figure 2 Flow chart of proteomics detection and analysis. A: Sprague-Dawley rat; B: Protein extraction of colon tissue; C: Protein enzymatic digestion, peptide labelling, separation, and high-performance liquid chromatography analysis; D: Bioinformatics analysis.

RESULTS

Effects of HM and EA on DSS induced UC rats

In the N group, rats were active and energetic, and their feces were moderately hard and soft. The rats in the M group had loose, bloody stools and decreased activities. Compared with the M group, the activity of rats in the HM and EA groups was obviously improved, and the stool gradually took shape without obvious mucus and blood. We found that the colon in the N group did not exhibit adhesion or bleeding points; the colonic mucosal surfaces were clean and smooth. In contracts, the colon in the M group exhibited significant adhesion and multiple bleeding points; the inner wall was not smooth, and partially visible scattered ulcers and thickened intestinal walls were observed. In the HM and EA groups, the adhesion and the bleeding points were decreased (Figure 3A).

The morphological changes of colon tissues were observed using HE staining. The colonic mucosal epithelium of the normal group was intact, with clear tissue structure, regular arranged glands, and no congestion, oedema or ulcers were evident. While the mucosal epithelium of UC rats was absent, ulcers had formed, with a loss or reduction of glands and goblet cells, and substantial inflammatory cells were infiltrated in mucosa and submucosa. After HM and EA interventions, the mucosal epithelium was restored, with healed ulcer, increased glands and goblet cells, decreased mucosal and submucosal inflammatory cell infiltration and congestion (Figure 3B).

The macroscopic colon injury scores and histopathology scores in the M group were significantly increased than that in the N group ($P < 0.01$). Conversely, the macroscopic colon injury scores and histopathology scores in the HM and EA groups were significantly decreased compared to the rats in the M group ($P < 0.01$) (Figures 3C and D). The colonic length of the rats in the M group were significantly decreased compared with the N group, the colonic length of the rats in the HM and EA groups were significantly increased compared with the M group ($P < 0.01$) (Figure 3E).

iTRAQ quantification of DEPs

The volcano plot in Figure 4 described the DEPs between the groups. The quantitative results showed that 202 DEPs were identified in DSS-induced UC rats compared with the N group, of which 111 were up-regulated and 91 were down-regulated; 117 DEPs were identified in HM group compared with the M group, of which 41 were up-regulated and 76 were down-regulated; 145 DEPs were identified in EA group compared with the M model group, of which 59 were up-regulated and 86 were down-regulated (Table 1, Figure 5).

Comparison of the M/N and HM/M groups showed that among these proteins, 25 DEPs were common to N, M and HM groups, with 17 [Sv2a, Igkv13-85, Ncbp1, Aldo-keto reductase family 1 member B8, Rathemoglobin beta-chain, Ribosomal protein S8 (RpS8), Fga, Rps2-ps6, carbamoyl phosphate synthetase 1 (Cps1), Txn, ATP synthase subunit g (ATP5L), Cox4i1, Atp5h, Necap2, Atp5f1, Papss2, Acly] up-regulated in UC but were down-regulated by HM, and 8 [Spout1, calcium-activated chloride channel regulator 1 (CLCA1), Sval1, Hspb7, Peptidyl-prolyl cis-trans isomerase, Aldh1a1, Lyz2, Dclk3] down-regulated in UC but were up-regulated by HM (Figure 5A, Table 2). Comparison of the M/N and EA/M groups showed that 15 DEPs were common to N, M and EA groups, with 9 (Sv2a, Ncbp1, Rat hemoglobin beta-chain, Fga, Cps1, ATP5L, Cox4i1, Atp5f1, Lmod1) up-regulated in UC but were down-regulated by EA, and 6 (Spout1, Sh3bgrl3, Peptidyl-prolyl cis-trans isomerase, MHC class I RT1.Aw3 protein, Tkt, Dclk3) down-regulated in UC but were up-regulated by EA (Figure 5B, Table 3).

GO enrichment analysis for DEPs

GO annotation of DEPs between groups describes the characteristics of genes and gene products in terms of molecular functions, cellular components and biological processes. 53 GO functions were significantly differentiated between the M and the N group, 52 GO functions are significantly differentiated between the M group and the HM group, and 51 GO functions are significantly differentiated between the M group and the EA group. The GO functional annotations of DEPs in the M/N, HM/M, and EA/M comparisons were basically similar. Biological process was the most favorable enrichment component, in which DEGs were significantly enriched in cellular process, metabolic process, biological regulation and so on. Cellular component analysis was enriched in cell part, cell, organelles, macromolecular complexes, *etc.* Molecular functions mainly included binding, synaptic activity, structural molecule activity, molecular function regulation, molecular sensor activity, and transcriptional regulation activity (Figure 6).

KEGG pathway enrichment analysis for DEPs

KEGG pathway enrichment analysis was performed for DEPs between the groups, we found that these DEPs were mainly enriched in inflammation responses and immune-related pathways. The pathways in which DEPs between the N and M groups mainly enriched included primary immunodeficiency, the noncanonical nuclear factor-kappaB (NF-κB) signalling pathway, natural killer cells mediated cytotoxicity, intestinal immune network for immunoglobulin A (IgA) production, FcγR-mediated phagocytosis, and complement and coagulation cascades (Figure 7A, Table 4). The pathways in which DEPs between the HM and the M groups mainly enriched included primary immunodeficiency,

Table 1 List of differential protein numbers

Compare group	Up-regulated	Down-regulated	All-regulated
M/N	111	91	202
HM/M	41	76	117
EA/M	59	86	145

N: Normal group; M: Dextran sulfate sodium-induced ulcerative colitis model group; HM: Herb-partitioned moxibustion group; EA: Electroacupuncture group.

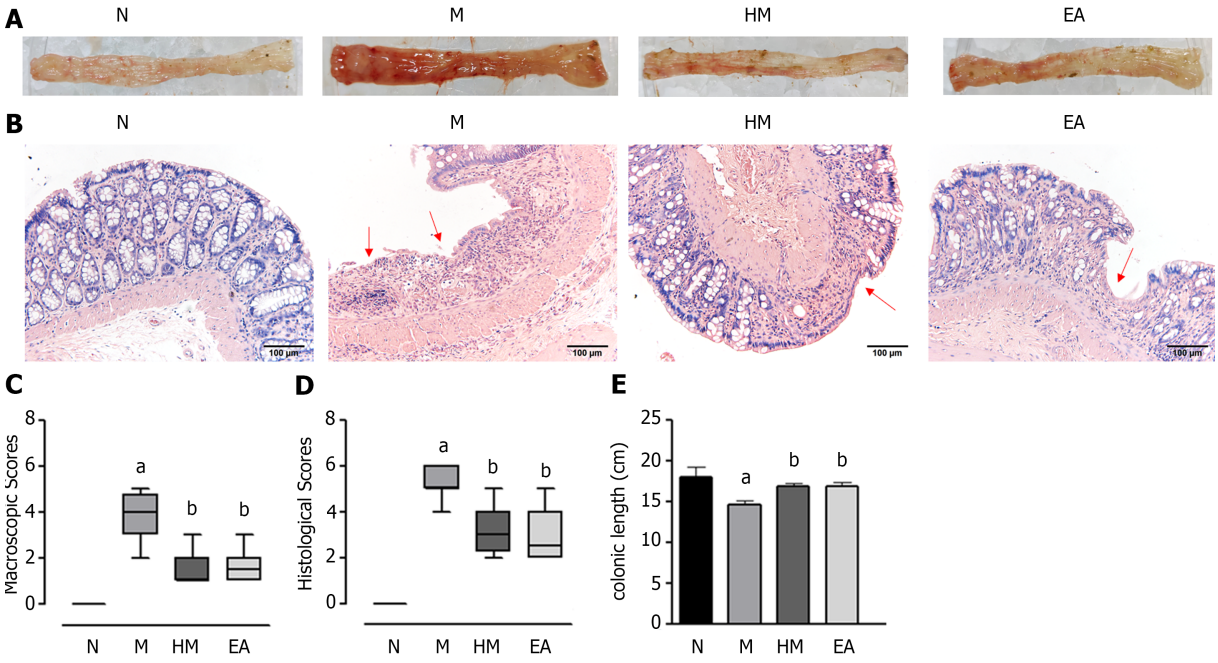

Figure 3 Colon tissue injuries in each group. A: Gross structure; B: Histopathological observation (hematoxylin and eosin, × 200); C: Macroscopic scores; D: Histopathological scores; E: Colonic length. $^{a}P < 0.01$ *vs* N group; $^{b}P < 0.01$ *vs* M group. N: Normal group; M: Dextran sulfate sodium-induced ulcerative colitis model group; HM: Herb-partitioned moxibustion group; EA: Electroacupuncture group.

oxidative phosphorylation, nitrogen metabolism, natural killer cells mediated cytotoxicity, the intestinal immune network for IgA production, FcγR-mediated phagocytosis, complement and coagulation cascades, and B cell receptor signalling pathway (Figure 7B, Table 5). The pathways in which DEPs between the EA and the M groups mainly enriched included the phosphoinositol-3 kinase (PI3K)-protein kinase B (Akt) signalling pathway, oxidative phosphorylation, intestinal immune network for IgA production, and the calcium signalling pathway (Figure 7C, Table 6).

Protein-protein interactions analysis

The STRING database (v.11.0) was used to construct the protein-protein interactions (PPIs) network for the transcription factors with an interaction score > 0.7 (high confidence) among the groups. Cytoscape (v.3.7.1) software was used to visualize the enrichment results. The statistical significance was set as $P < 0.05$. The analysis showed extensive interactions among the DEPs between groups (Figure 8). A total of 100 DEPs (63 up-regulated proteins and 37 down-regulated proteins) were included in the PPI network constructed by DEPs between the N and M groups, and Nme2 served as the junction point of two pathways, indicating that it was important for screening key candidate proteins. 38 DEPs (8 up-regulated proteins and 30 down-regulated proteins) were included in the PPI network constructed from DEPs between the M and HM groups, in which ribosomal pathway-related proteins were all down-regulated, and oxidative phosphorylation pathway-related proteins, including Atp5o, ATP5L, Atp5f, Atp5h, Cox4i1 were also down-regulated. 55 DEPs (19 up-regulated proteins and 36 down-regulated proteins) were included in the PPI network constructed from DEPs between the EA and M groups. In addition, proteins involved in inflammation regulation such as serpins were identified (serpinb6 in M/N comparisons, serpinc1 in HM/M and EA/M comparisons).

Table 2 Differentially expressed proteins in dextran sulfate sodium-induced ulcerative colitis model group rats that regulated by herb-partitioned moxibustion

Protein ID	Description	Symbol	M/N		HM/M	
			Mean ratio	Q value	Mean ratio	Q value
Q02563	Synaptic vesicle glycoprotein 2A	Sv2a	4.42	0.024	0.25	0.021
A0A0G2JZN1	Immunoglobulin kappa chain variable 13-85	Igkv13-85	4.07	0.020	0.37	0.028
Q56A27	Nuclear cap-binding protein subunit 1	Ncbp1	2.47	0.018	0.56	0.004
Q91W30	Aldose reductase-like protein	Akr1b8	1.85	0.006	0.63	0.017
Q63223	Rat hemoglobin beta-chain (Fragment)	Rat hemoglobin beta-chain (Fragment)	1.57	0.005	0.46	0.004
P62243	40S ribosomal protein S8	Rps8	1.56	0.006	0.83	0.023
P06399	Fibrinogen alpha chain	Fga	1.51	0.003	0.75	0.004
O55215	Ribosomal protein S2	Rps2-ps6	1.45	0.003	0.80	0.004
P07756	Carbamoyl-phosphate synthase (ammonia), mitochondrial	Cps1	1.33	0.009	0.70	0.004
P11232	Thioredoxin	Txn	1.28	0.002	0.74	0.004
Q6PDU7	ATP synthase subunit g, mitochondrial	ATP5L	1.27	0.028	0.76	0.004
P10888	Cytochrome c oxidase subunit 4 isoform 1, mitochondrial	Cox4i1	1.26	0.002	0.80	0.004
P31399	ATP synthase subunit d, mitochondrial	Atp5h	1.34	0.003	0.77	0.004
Q6P756	Adaptin ear-binding coat-associated protein 2	Necap2	1.48	0.011	0.83	0.023
P19511	ATP synthase F (0) complex subunit B1, mitochondrial	Atp5f1	1.24	0.003	0.83	0.004
A0A0G2K950	3′-phosphoadenosine 5′-phospho-sulfate synthase 2	Papss2	1.27	0.002	0.74	0.004
A0A0G2K5E7	ATP-citrate synthase	Acly	1.35	0.017	0.83	0.030
A0A0G2QC59	RCG45649, isoform CRA_a	Spout1	0.54	0.013	2.13	0.011
A0A0G2JWX9	Chloride channel accessory 1	Clca1	0.50	0.002	1.25	0.004
Q99N82	Colon SVA-like protein	Sval1	0.73	0.028	6.82	0.004
B5DFG4	Heat shock 27kD protein family, member 7 (cardiovascular)	Hspb7	0.76	0.016	1.24	0.050
D3ZSF3	Peptidyl-prolyl cis-trans isomerase	-	0.75	0.003	1.40	0.013
P51647	Retinal dehydrogenase 1	Aldh1a1	0.81	0.002	1.22	0.004
Q05820	Putative lysozyme C-2	Lyz2	0.67	0.013	1.48	0.050
F1LWF2	Doublecortin-like kinase 3	Dclk3	0.24	0.005	4.67	0.011

N: Normal group; M: Dextran sulfate sodium-induced ulcerative colitis model group; HM: Herb-partitioned moxibustion group; ATP5L: ATP synthase subunit g; Atp5f1: ATP synthase beta subunit precursor; Sv2a: Synaptic vesicle glycoprotein 2A; Ncbp1: Nuclear cap binding protein subunit 1; Cps1: Carbamoyl phosphate synthetase 1; Cox4i1: Cytochrome c oxidase subunit 4 isoform 1; Dclk3: Doublecortin like kinase 3; Akr1b8: Aldo-keto reductase family 1 member B8; RpS8: Ribosomal protein S8.

Western blot verification

We verified the expression of some DEPs that could be regulated by HM and EA. The western blot results showed that, compared with the N group, the expression of Sv2a, Ncbp1, Cps1, Cox4i1, Atp5f1 proteins were increased in the colon of UC rats, while the expression of Dclk3 protein was decreased ($P < 0.01$). HM and EA interventions can significantly down-regulate the expression of Sv2a, Ncbp1, Cps1, Cox4i1, Atp5f1 proteins and up-regulate Dclk3 protein ($P < 0.01$). It indicated that the western blot

Table 3 Differentially expressed proteins in dextran sulfate sodium-induced ulcerative colitis model group rats that regulated by electroacupuncture

Protein ID	Description	Symbol	M/N		EA/M	
			Mean ratio	Q value	Mean ratio	Q value
Q02563	Synaptic vesicle glycoprotein 2A	Sv2a	4.42	0.024	0.15	0.013
Q56A27	Nuclear cap-binding protein subunit 1	Ncbp1	2.47	0.018	0.55	0.003
Q63223	Rat hemoglobin beta-chain (Fragment)	-	1.57	0.005	0.38	0.002
P06399	Fibrinogen alpha chain	Fga	1.51	0.003	0.76	0.002
P07756	Carbamoyl-phosphate synthase (ammonia), mitochondrial	Cps1	1.33	0.009	0.69	0.004
Q6PDU7	ATP synthase subunit g, mitochondrial	ATP5L	1.27	0.028	0.82	0.002
P10888	Cytochrome c oxidase subunit 4 isoform 1, mitochondrial	Cox4i1	1.26	0.002	0.74	0.002
P19511	ATP synthase F (0) complex subunit B1, mitochondrial	Atp5f1	1.51	0.003	0.81	0.002
A0A0G2K0D3	Leiomodin-1	Lmod1	1.13	0.003	0.77	0.002
A0A0G2QC59	RCG45649, isoform CRA_a	Spout1	0.54	0.013	1.88	0.002
B2RZ27	SH3 domain binding glutamic acid-rich protein-like 3	Sh3bgrl3	0.74	0.027	1.31	0.027
D3ZSF3	Peptidyl-prolyl cis-trans isomerase	-	0.75	0.003	1.47	0.003
Q31266	MHC class I RT1.Aw3 protein	-	0.81	0.029	1.44	0.005
G3V826	Transketolase OS = rattus norvegicus	Tkt	0.71	0.003	1.23	0.002
F1LWF2	Doublecortin-like kinase 3	Dclk3	0.24	0.005	4.09	0.002

N: Normal group; M: Dextran sulfate sodium-induced ulcerative colitis model group; EA: Electroacupuncture group; ATP5L: ATP synthase subunit g; Atp5f1: ATP synthase beta subunit precursor; Sv2a: Synaptic vesicle glycoprotein 2A; Ncbp1: Nuclear cap binding protein subunit 1; Cps1: Carbamoyl phosphate synthetase 1; Cox4i1: Cytochrome c oxidase subunit 4 isoform 1; Dclk3: Doublecortin like kinase 3.

verification results were consistent with the iTRAQ results (Figure 9).

DISCUSSION

UC is a type of inflammatory bowel disease (IBD) characterized by chronic recurrent, and the specific aetiology and pathogenesis of UC are still not clear. Proteomics is a discipline that systematically quantifies all the proteins in cells or organisms and elucidates their biological functions, it has enormous potential for early diagnosis, prevention, and prognosis prediction of diseases[17,18]. In recent years, proteomics has gradually been applied to the study of UC, providing strong support for the research of pathogenesis, clinical diagnosis, and treatment of UC. A study has been found that 7 protein genes were differentially expressed in the intestinal tissues of UC patients using proteomics, including prohibitin, heat shock proteins, alpha-1 antitrypsin, ventralis intermedius, caspase-1, cytokeratin 20, Filamin Ainteracting protein 1, FLNa[19]. Another study analysed the transcriptome and proteome characteristics of the colon of UC patients, and found that the expression of genes and proteins related to immune and inflammatory responses in UC patients were dysregulated. At the same time, the complement cascade, metabolic processes, and peroxisome proliferator-activated receptor signal transduction were inhibited[20]. Therefore, iTRAQ proteomic technology can also be a feasible method to reveal potential targets for UC drug therapy[8].

In the present study, we performed proteomic analysis using iTRAQ labelling combined with mass spectrometry technology to identify DEPs in colon of DSS-induced UC rats, and selected DEPs that could be reversed by HM and EA. DSS has been widely used to prepare experimental colitis to study the new drug therapy, immunity and mechanism of action[21-23]. Our results showed that HM and EA improved the colonic mucosal injury of UC rats. At the same time, we have compared the normal and

Table 4 The Kyoto Encyclopedia of Genes and Genomes pathway related to immunity and inflammation with differentially expressed proteins between normal group and dextran sulfate sodium-induced ulcerative colitis model group

Pathway name	Protein ID	Number	*P* value
Primary immunodeficiency	M0RDF2, IGG2B, M0RA79, Q4QQW0, F1LXY6, Q569B3	6	0.003
Nuclear factor-kappa B signalling pathway	M0RDF2, IGG2B, M0RA79, Q4QQW0, F1LXY6, Q569B3, B2RZB2	7	0.021
Natural killer cell mediated cytotoxicity	GRZ2, M0RDF2, IGG2B, M0RA79, Q4QQW0, F1LXY6, Q569B3	7	0.025
Intestinal immune network for IgA production	M0RDF2, IGG2B, HB2B, M0RA79, Q8VI32, Q4QQW0, F1LXY6, Q569B3, B2RZB2	9	4.25E-05
Fc gamma R-mediated phagocytosis	M0RDF2, Q6AYB2, IGG2B, E9PU64, M0RA79, Q4QQW0, F1LXY6, B2GV73, Q569B3	9	0.007
Complement and coagulation cascades	CFAI, FIBB, M0RBJ7, PLMN, A1L114, CO9, A1M, FIBG, FIBA, Q99N82, A0A0G2JY31	11	8.29E-06

N: Normal group; M: Dextran sulfate sodium-induced ulcerative colitis model group; IgA: Immunoglobulin A.

Table 5 The Kyoto Encyclopedia of Genes and Genomes pathway related to immunity, inflammation and oxidative phosphorylation with differentially expressed proteins between herb-partitioned moxibustion group and dextran sulfate sodium-induced ulcerative colitis model group

Pathway name	Protein ID	Number	*P* value
Primary immunodeficiency	IGG2C, Q5BJZ2, F1LXY6, Q569B3	4	0.009
Oxidative phosphorylation	ATP5H, ATPO, COX41, AT5F1, Q5UAJ5, NMES1, ATP5L	7	0.002
Nitrogen metabolism	CAH1, CAH3, CPSM	3	0.001
Natural killer cell mediated cytotoxicity	GRZ2, IGG2C, Q5U1Y2, Q5BJZ2, F1LXY6, Q569B3	6	0.005
Intestinal immune network for IgA production	IGG2C, Q5BJZ2, Q6MG98, F1LXY6, Q569B3	5	0.002
Fc gamma R-mediated phagocytosis	IGG2C, Q5U1Y2, Q5BJZ2, F1LXY6, Q569B3	5	0.040
Complement and coagulation cascades	Q5M7T5, Q99N82, Q7TQ70, FIBA	4	0.031
B cell receptor signalling pathway	IGG2C, Q5U1Y2, Q5BJZ2, F1LXY6, Q569B3	5	0.020

M: Dextran sulfate sodium-induced ulcerative colitis model group; HM: Herb-partitioned moxibustion group; IgA: Immunoglobulin A; ATP5L: ATP synthase subunit g.

Table 6 The Kyoto Encyclopedia of Genes and Genomes pathway related to immunity, inflammation and oxidative phosphorylation with differentially expressed proteins between electroacupuncture group and dextran sulfate sodium-induced ulcerative colitis model group

Pathway name	Protein ID	Number	*P* value
PI3K-Akt signalling pathway	F1M6Q3, D4A3K7, P70570, Q5M7V3, A0A096P6L8, Q5BJZ2, F1LPR6, GBB4, PCKGC	9	0.042
Oxidative phosphorylation	B2RYT5, CX7A2, D4A565, CX6C2, COX41, M0RA24, AT5F1, B2RYS8, G3V8S4, D3ZFQ8, NMES1, ATP5L, ATPK	13	3.42E-07
Intestinal immune network for IgA production	Q5M7V3, Q5BJZ2, F1LPR6, Q6MG98	4	0.032
Calcium signalling pathway	GNAS2, Q5M7V3, A0A0G2K059, Q5BJZ2, F1LPR6, A0A0G2JSR0, ADT2	7	0.027

M: Dextran sulfate sodium-induced ulcerative colitis model group; EA: Electroacupuncture group; IgA: Immunoglobulin A; ATP5L: ATP synthase subunit g; PI3K-Akt: Phosphatidylinositol 3-kinase protein kinase B; COX41: Cytochrome c oxidase subunit IV isoform 1; PCKGC: Phosphoenolpyruvate carboxykinase 1; ATPK: ATP synthase membrane subunit F; ADT2: Arogenate dehydratase 2.

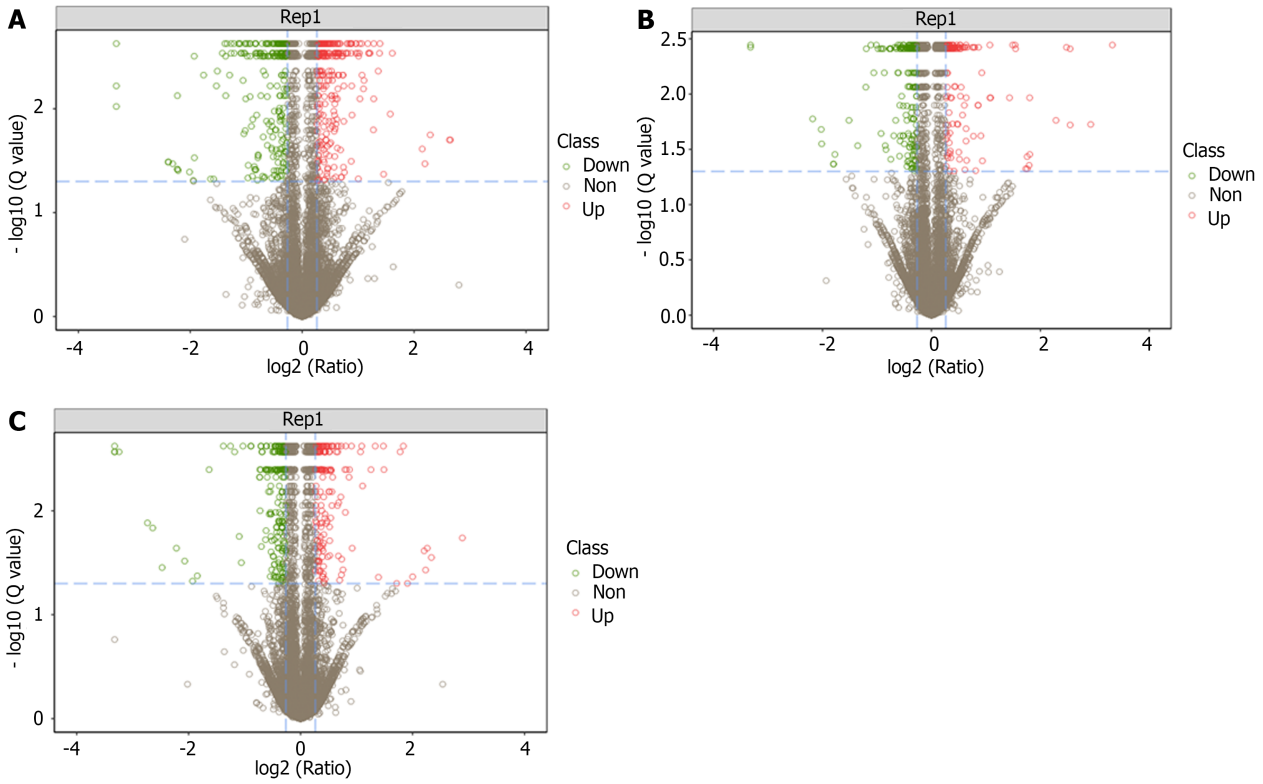

Figure 4 Volcano plot of differentially expressed proteins between groups. A: Volcano plot of differentially expressed proteins (DEPs) between the normal and dextran sulfate sodium-induced ulcerative colitis model group; B: Volcano plot of DEPs between the dextran sulfate sodium-induced ulcerative colitis model and herb-partitioned moxibustion group; C: Volcano plot of DEPs between the dextran sulfate sodium-induced ulcerative colitis model and electroacupuncture group.

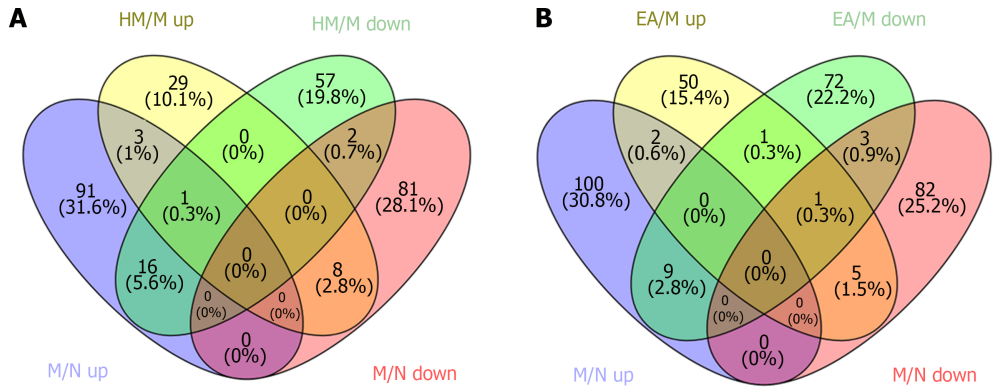

Figure 5 Venn diagram of differentially expressed proteins among groups. A: Venn diagram of differentially expressed proteins (DEPs) in dextran sulfate sodium-induced ulcerative colitis model group that can be regulated by herb-partitioned moxibustion; B: Venn diagram of DEPs in dextran sulfate sodium-induced ulcerative colitis model group that can be regulated by electroacupuncture. N: Normal group; M: Dextran sulfate sodium-induced ulcerative colitis model group; HM: Herb-partitioned moxibustion group; EA: Electroacupuncture group.

DSS-induced UC rats using iTRAQ labelling and found that 202 protein genes were differentially expressed between the two group. Among them, galectin-3, an up-regulated protein, is an endogenous lectin with extensive immunomodulatory functions, and can promote the inflammatory response in DSS-induced colitis by activating the NLR family pyrin domain containing 3 inflammasome[24]. Moreover, galectin-3 has also been shown to be a key regulator of inflammation and can be a potential biomarker for IBD[25]. s100a9 is a subunit of calprotectin with pro-inflammatory activity, and the level of s100a9 was significantly increased in the faeces of DSS-induced colitis mice compared with normal mice[26,27]. This is consistent with the upregulation of s100a9 in UC colon tissue in our study. Guanylate cyclase activator 2A (GUCA2A) is the ligand of guanylate cyclase C, which is mainly expressed in intestinal epithelial cells, and can regulate intestinal barrier function and intestinal homeostasis through the cyclic guanosine monophosphate-dependent signalling pathway[28]. The

A

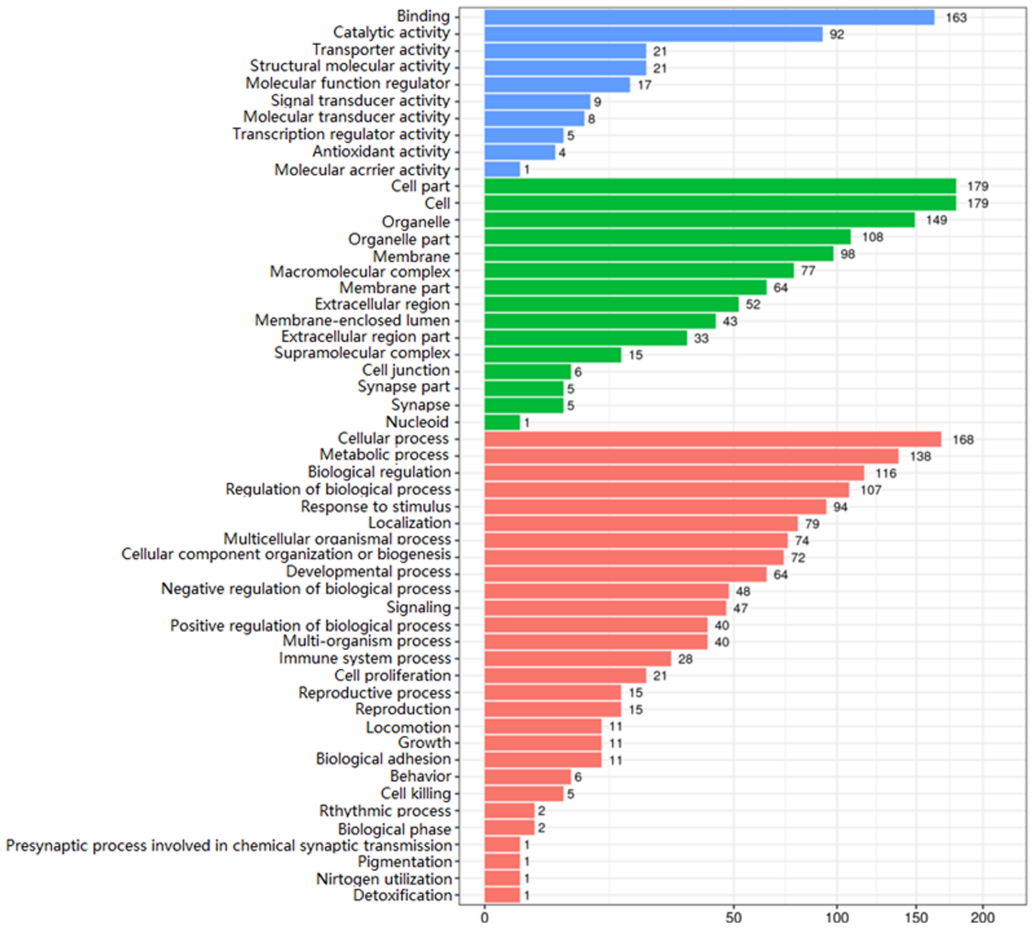
Binding 163
Catalytic activity 92
Transporter activity 21
Structural molecular activity 21
Molecular function regulator 17
Signal transducer activity 9
Molecular transducer activity 8
Transcription regulator activity 5
Antioxidant activity 4
Molecular acrrier activity 1
Cell part 179
Cell 179
Organelle 149
Organelle part 108
Membrane 98
Macromolecular complex 77
Membrane part 64
Extracellular region 52
Membrane-enclosed lumen 43
Extracellular region part 33
Supramolecular complex 15
Cell junction 6
Synapse part 5
Synapse 5
Nucleoid 1
Cellular process 168
Metabolic process 138
Biological regulation 116
Regulation of biological process 107
Response to stimulus 94
Localization 79
Multicellular organismal process 74
Cellular component organization or biogenesis 72
Developmental process 64
Negative regulation of biological process 48
Signaling 47
Positive regulation of biological process 40
Multi-organism process 40
Immune system process 28
Cell proliferation 21
Reproductive process 15
Reproduction 15
Locomotion 11
Growth 11
Biological adhesion 11
Behavior 6
Cell killing 5
Rthythmic process 2
Biological phase 2
Presynaptic process involved in chemical synaptic transmission 1
Pigmentation 1
Nirtogen utilization 1
Detoxification 1
0
50
100
150
200

B

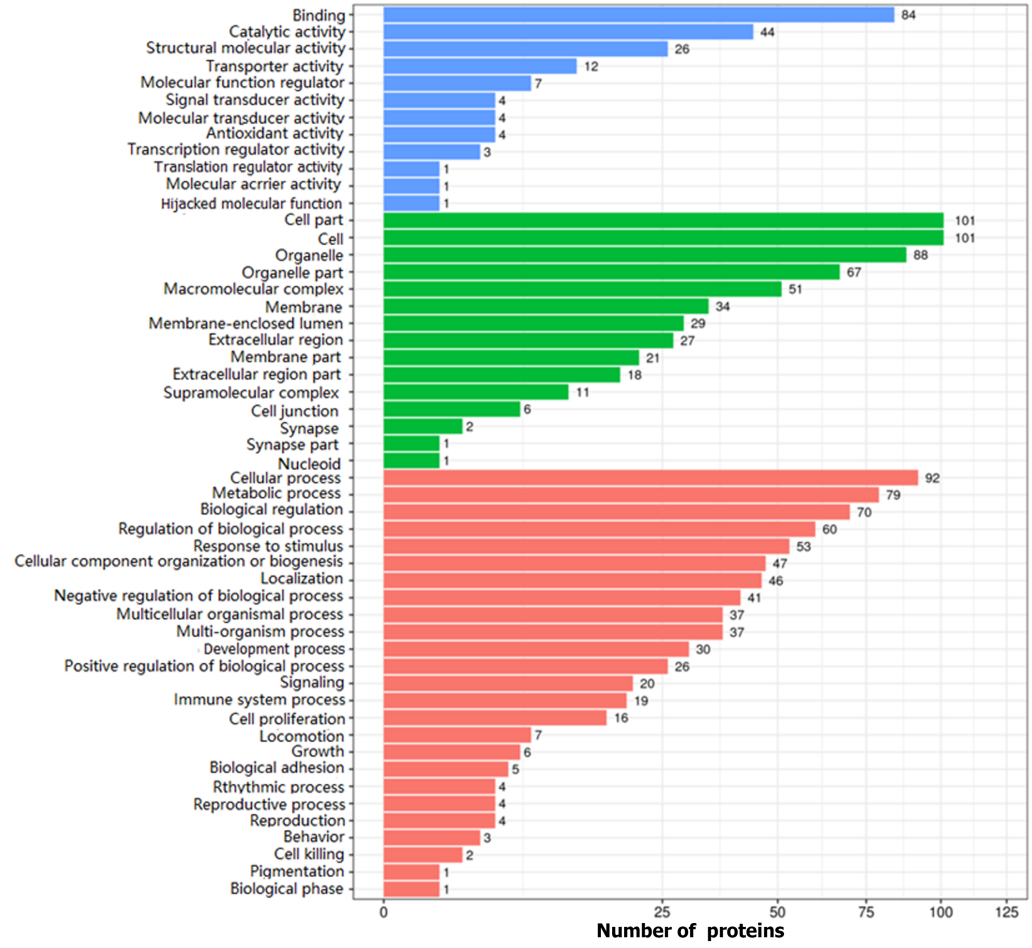
Binding 84
Catalytic activity 44
Structural molecular activity 26
Transporter activity 12
Molecular function regulator 7
Signal transducer activity 4
Molecular transducer activity 4
Antioxidant activity 4
Transcription regulator activity 3
Translation regulator activity 1
Molecular acrrier activity 1
Hijacked molecular function 1
Cell part 101
Cell 101
Organelle 88
Organelle part 67
Macromolecular complex 51
Membrane 34
Membrane-enclosed lumen 29
Extracellular region 27
Membrane part 21
Extracellular region part 18
Supramolecular complex 11
Cell junction 6
Synapse 2
Synapse part 1
Nucleoid 1
Cellular process 92
Metabolic process 79
Biological regulation 70
Regulation of biological process 60
Response to stimulus 53
Cellular component organization or biogenesis 47
Localization 46
Negative regulation of biological process 41
Multicellular organismal process 37
Multi-organism process 37
Development process 30
Positive regulation of biological process 26
Signaling 20
Immune system process 19
Cell proliferation 16
Locomotion 7
Growth 6
Biological adhesion 5
Rthythmic process 4
Reproductive process 4
Reproduction 4
Behavior 3
Cell killing 2
Pigmentation 1
Biological phase 1
0
25
50
75
100
125
Number of proteins

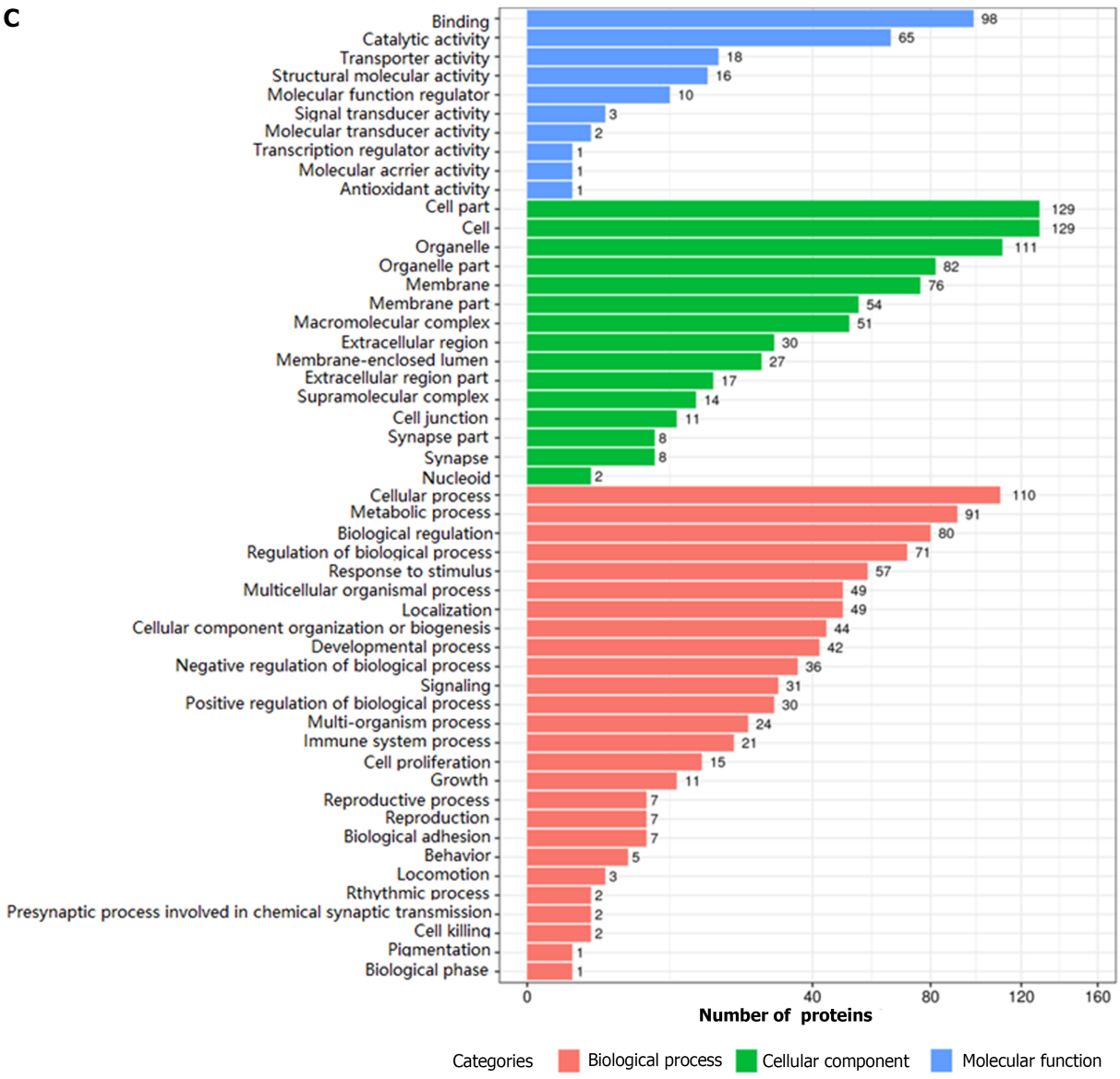

Figure 6 Biological function annotation of differentially expressed proteins between groups. A: Biological function annotation of differentially expressed proteins (DEPs) between the normal and dextran sulfate sodium-induced ulcerative colitis model group; B: Biological function annotation of DEPs between the dextran sulfate sodium-induced ulcerative colitis model and herb-partitioned moxibustion group; C: biological function annotation of DEPs between the dextran sulfate sodium-induced ulcerative colitis model and electroacupuncture group.

down-regulation of GUCA2A can injure the intestinal mucosa barrier and affect the growth and repair of intestinal epithelial cells in IBD patients[29]. Interestingly, we found that the expression of GUCA2A was down-regulated in UC colon tissue, which was consistent with previous findings. These results suggest that galectin-3, s100a9 and GUCA2A may be potential biomarkers of UC.

After receiving the HM intervention, a total of 117 DEPs were identified, of which 25 proteins were reversely regulated by HM, including 17 proteins up-regulated in UC but were down-regulated by HM, and 8 down-regulated in UC but were up-regulated by HM. Among the 17 proteins down-regulated by HM, ATP5L, Atp5f, and Atp5h are the subunits of ATP synthase that involved in energy metabolism and oxidative phosphorylation; Cox4i1 is an important regulatory subunit of cytochrome c oxidase and is mainly associated with mitochondrial oxidative phosphorylation; Cps1, the carbamyl phosphate synthetase 1, was over-expressed in the non-dysplastic tissue of UC progressors[30]; RpS8 is a small subunit protein of ribosomes that plays a critical role in regulation of protein translation. Although it is unclear whether these proteins play a role in UC, ATP-induced energy metabolism disorders and intestinal epithelial mitochondrial damage are important pathogenesis of UC[31]. Therefore, changes in the expression of these proteins may be related to the occurrence of UC and the therapeutic effect of HM. Further studies should be performed to clarify the exact mechanisms of these oxidative phosphorylation proteins. Among the 8 proteins up-regulated by HM, CLCA1 is one of the major non-mucinous proteins in intestinal mucus, which is normally expressed in the gastrointestinal tract and is most abundant in the intestinal mucosa. Studies have shown that CLCA1 regulates the structural

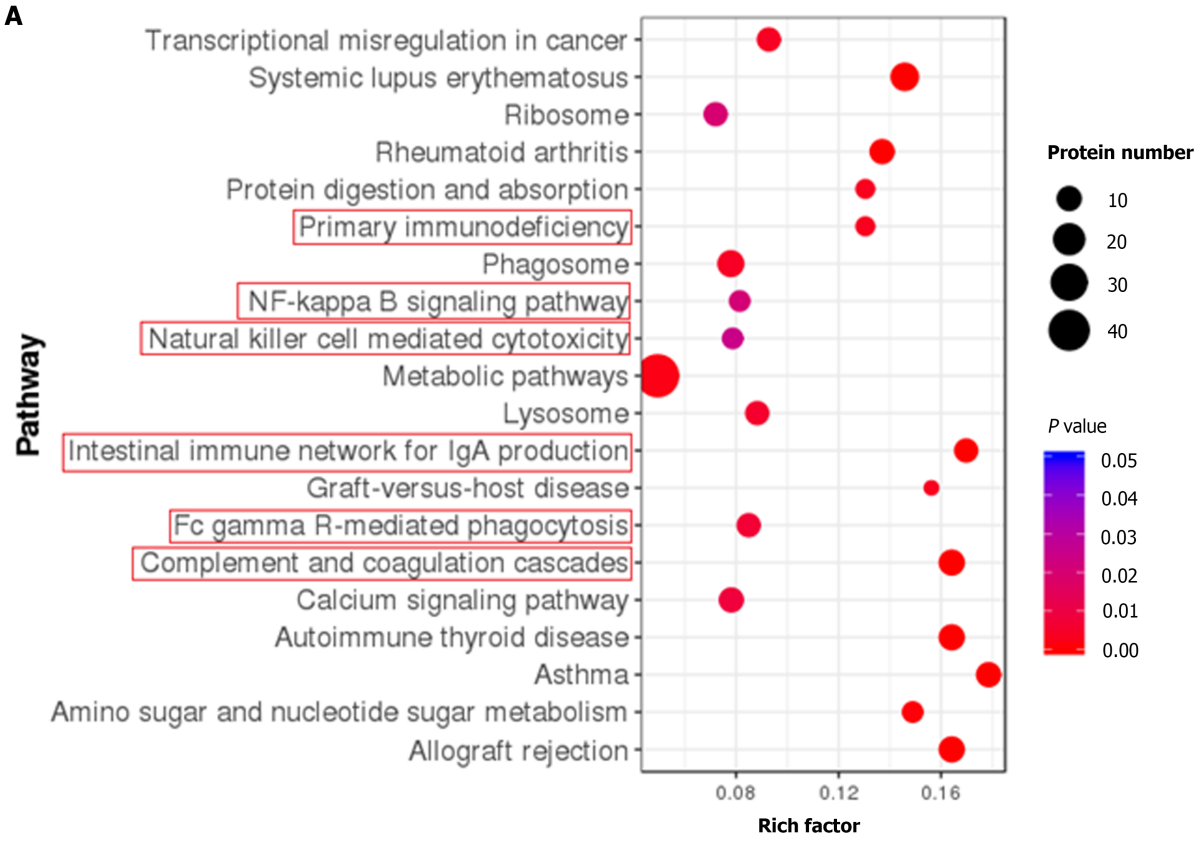
A
Transcriptional misregulation in cancer
Systemic lupus erythematosus
Ribosome
Rheumatoid arthritis
Protein digestion and absorption
Primary immunodeficiency
Phagosome
NF-kappa B signaling pathway
Natural killer cell mediated cytotoxicity
Metabolic pathways
Lysosome
Intestinal immune network for IgA production
Graft-versus-host disease
Fc gamma R-mediated phagocytosis
Complement and coagulation cascades
Calcium signaling pathway
Autoimmune thyroid disease
Asthma
Amino sugar and nucleotide sugar metabolism
Allograft rejection
Pathway
0.08
0.12
0.16
Rich factor
Protein number
10
20
30
40
P value
0.05
0.04
0.03
0.02
0.01
0.00

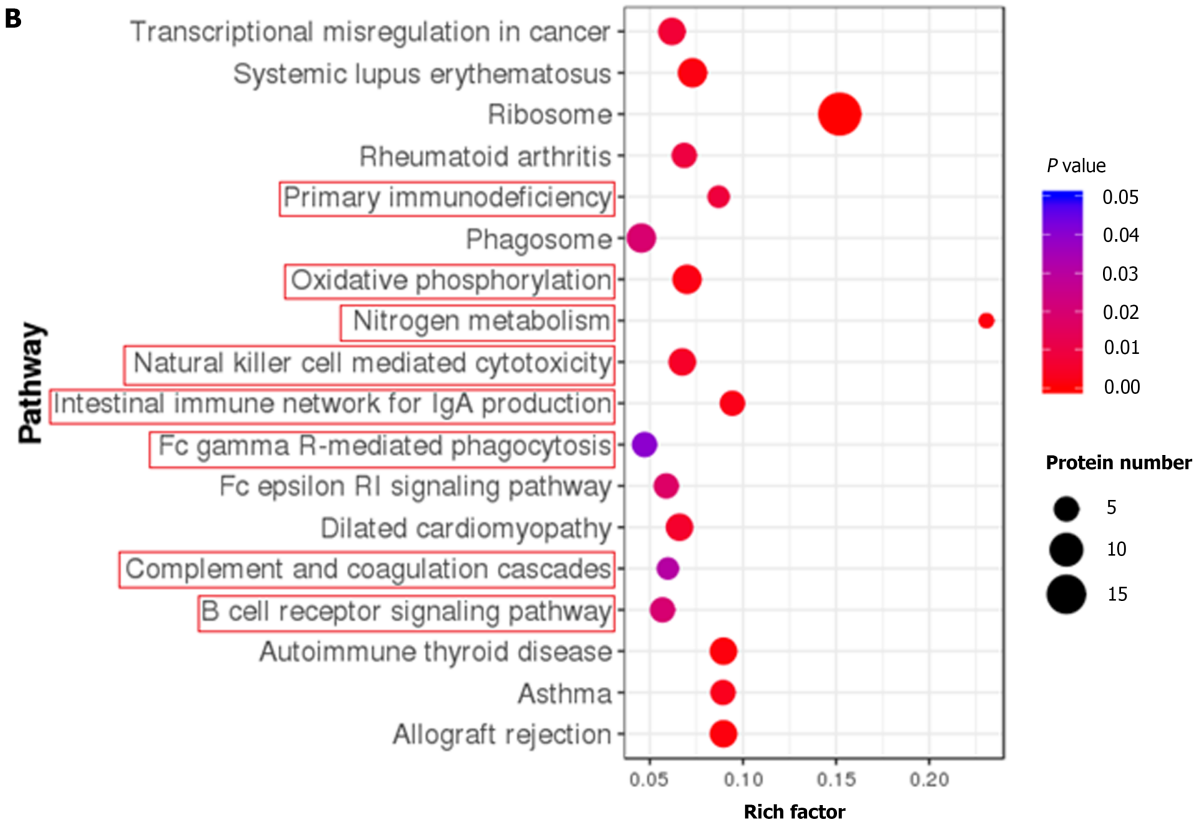
B
Transcriptional misregulation in cancer
Systemic lupus erythematosus
Ribosome
Rheumatoid arthritis
Primary immunodeficiency
Phagosome
Oxidative phosphorylation
Nitrogen metabolism
Natural killer cell mediated cytotoxicity
Intestinal immune network for IgA production
Fc gamma R-mediated phagocytosis
Fc epsilon RI signaling pathway
Dilated cardiomyopathy
Complement and coagulation cascades
B cell receptor signaling pathway
Autoimmune thyroid disease
Asthma
Allograft rejection
Pathway
0.05
0.10
0.15
0.20
Rich factor
P value
0.05
0.04
0.03
0.02
0.01
0.00
Protein number
5
10
15

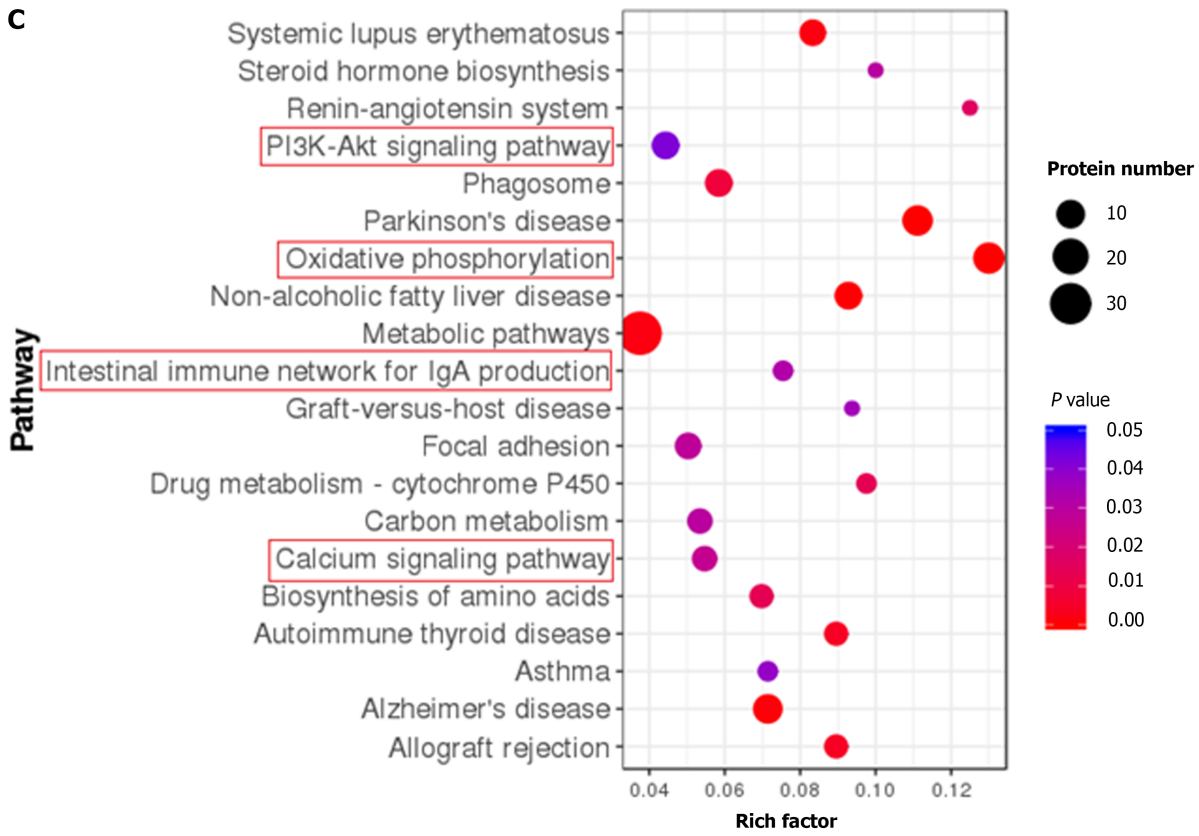

Figure 7 Kyoto Encyclopedia of Genes and Genomes pathway enrichment of differentially expressed proteins between groups. A: Kyoto Encyclopedia of Genes and Genomes (KEGG) pathway enrichment of differentially expressed proteins (DEPs) between the normal and dextran sulfate sodium-induced ulcerative colitis model group; B: KEGG pathway enrichment of DEPs between the dextran sulfate sodium-induced ulcerative colitis model and herb-partitioned moxibustion group; C: KEGG pathway enrichment of DEPs between the dextran sulfate sodium-induced ulcerative colitis model and electroacupuncture group. Each point in the KEGG pathway enrichment plot represents a KEGG pathway, with the left axis showing the pathway name and the abscissa showing the enrichment factor, which represents the ratio of the number of DEPs annotated to that pathway to the number of proteins annotated to that pathway for that species' protein. A larger enrichment factor indicates more reliable enrichment of DEPs in the pathway.

arrangement of mucus, participate in the mucus processing, and plays an important role in regulating intestinal homeostasis and intestinal inflammation[32-34]. CLCA1 can also exert a tumor suppressor effect in colorectal cancer (CRC) by inhibiting the Wnt/β-catenin signalling pathway and epithelial-mesenchymal transition process[35]. The serum concentration and mRNA expression of CLCA1 in CRC tissues were negatively correlated with metastasis and tumor staging[36,37]. These findings suggest that CLCA1 may play an important role in moxibustion in inhibiting the development and carcinogenesis of UC. While 15 proteins were reversely regulated by EA, of which 9 up-regulated in UC but were down-regulated by EA, and 6 down-regulated in UC but were up-regulated by EA. We found EA could also regulate the expression of Atp5f, Cox4i1, Cps1 that explained above, but the functions of other reversely regulated proteins in UC and immune inflammation remain unknown and require further validation and study.

We further explored the potential functions of DEPs by GO and KEGG functional enrichment analyses. GO analysis revealed that the majority of the DEPs were primarily involved in cellular process, metabolic process, biological regulation in biological processes, cell part, cell, organelles, macromolecular complexes in cellular component, and binding, synaptic activity, structural molecule activity, molecular function regulation, molecular sensor activity, and transcriptional regulation activity in molecular function. The results indicated that most differentially abundant proteins were associated with cell structure and catalytic activity which play an important role in cell function. For KEGG analysis, we found that these DEPs were mainly enriched in inflammation responses and immune-related pathways, such as primary immunodeficiency, NF-κB signalling pathway, natural killer cells mediated cytotoxicity, intestinal immune network for IgA production and so on. It has been confirmed that inflammatory response and immune response play an important role in UC. Numerous literature evidence that NF-κB pathway plays an essential role in pathogenic development of UC[38]. In addition, PPI network analysis showed that DEPs related to ribosomal pathways and oxidative phosphorylation pathways were all down-regulated by HM. As we all know that classical signalling pathways, such as the NF-κB signalling pathway, PI3K-Akt signalling pathway, have been confirmed to be associated with UC[39-42], and IgG receptor FcγR also plays an important role in UC intestinal immunity and inflam-

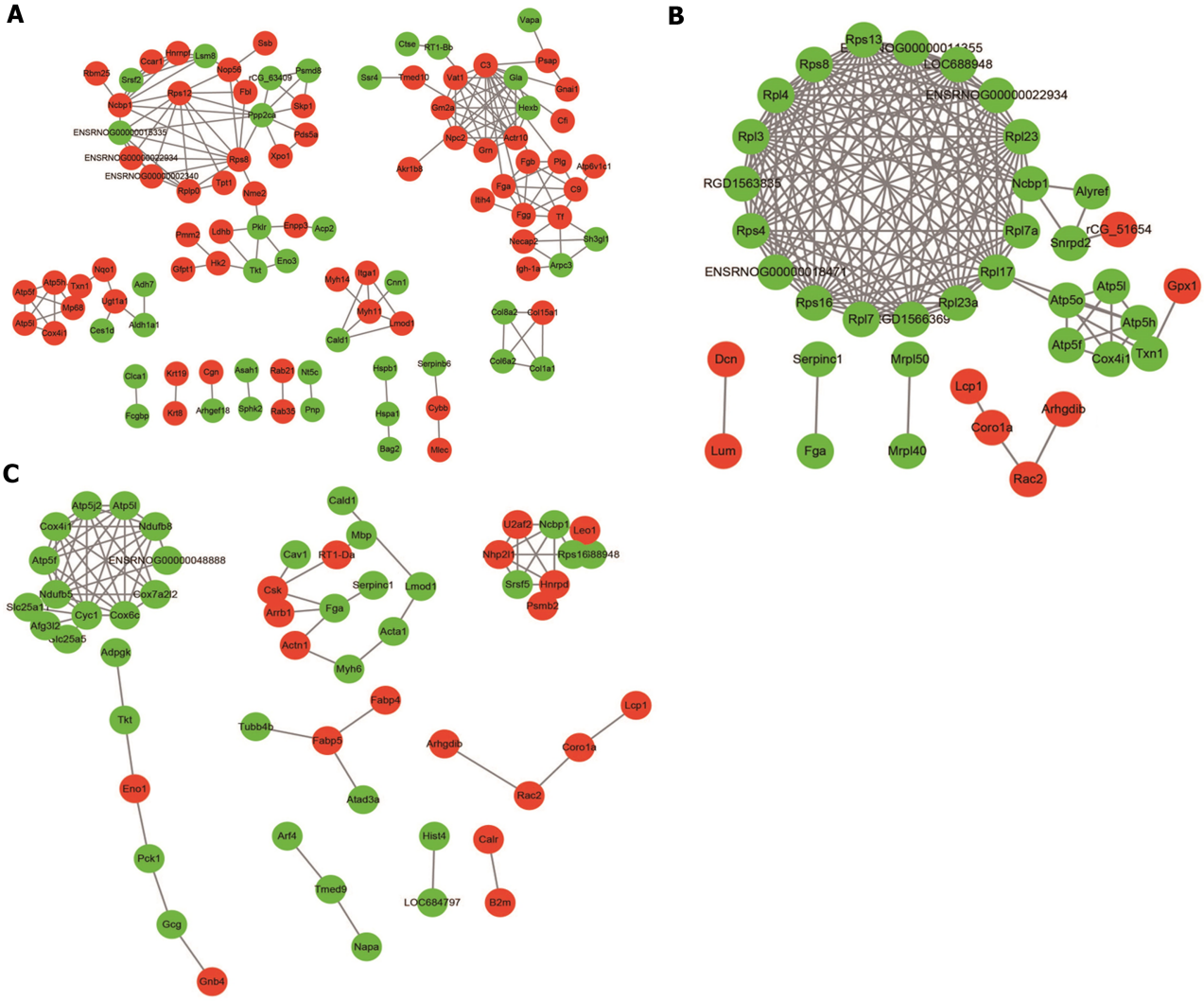

Figure 8 Protein-protein interaction network of differentially expressed proteins between groups. A: Protein-protein interaction (PPI) network of differentially expressed proteins (DEPs) between the normal and dextran sulfate sodium-induced ulcerative colitis model group; B: PPI network of DEPs between the dextran sulfate sodium-induced ulcerative colitis model and herb-partitioned moxibustion group; C: PPI network of DEPs between the dextran sulfate sodium-induced ulcerative colitis model and electroacupuncture group. Circle colours indicate changes in protein expression, with red indicating up-regulation and green indicating down-regulation, and line thickness indicates interaction intensity.

mation[43,44]. The intestinal immune network for IgA production and Fc epsilon RI signalling pathway may also the UC-specific signalling pathway. A study on pathway enrichment analysis of differentially expressed genes between IBD and healthy individuals revealed that primary immunodeficiency, complement and coagulation cascades, and nitrogen metabolism pathways may also play a key role in the progression of IBD[45]. Multiple algorithm analysis found that calcium signalling pathway was involved in the process of UC[46]. This is consistent with our findings at the protein level. Therefore, the abnormality of above pathways may be the key to the pathogenesis of UC, and HM and EA may play the therapeutic role in UC through the regulation of key molecules in these pathways. In addition, we found that proteins involved in inflammation regulation such as serpins were identified (serpinb6 in M/N comparisons, serpinc1 in HM/M and EA/M comparisons). Serpins are the largest known family of serine proteinase inhibitors, which regulate innate immunity by inhibiting the serine proteinase cascades that initiate immune responses such as melanization and antimicrobial peptide production [47]. Several human serpins have been shown to regulate serine proteases associated with processes such as inflammation and immune responses[48]. And increased activity of serine proteases is demonstrated in IBD patients and may contribute to the onset and the maintenance of the disease[49]. This appears to be a novel finding that will require additional research.

We also found that both HM and EA reversed the expression of Sv2a, Ncbp1, Rat hemoglobin beta-chain (Fragment), Fga, Cps1, ATP5L, Cox4i1, Atp5f1, Spout1, Peptidyl-prolyl cis-trans isomerase, Dclk3 proteins, while the rest is what they can reverse individually. The KEGG pathways of DEPs between HM and M groups, EA and M groups were also partly different. These results may reflect the commonness and characteristics of the therapeutic effects of HM and EA. So, the effects of HM and EA on UC may involve the differently regulating proteins and pathways. In addition, based on the results

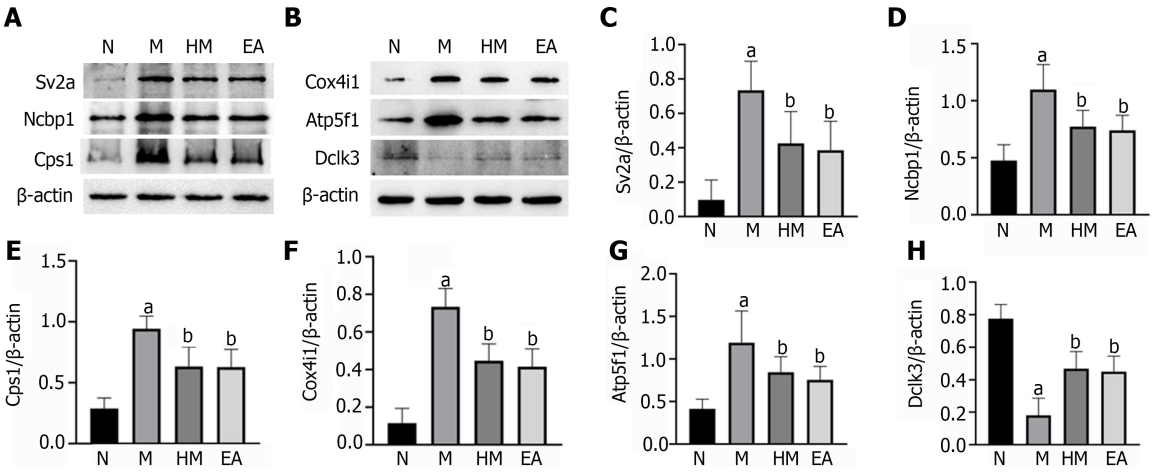

Figure 9 Verification of differentially expressed proteins expressions by western blot. A and B: Band diagrams of protein expressions. All data are expressed as mean ± SD; C: Synaptic vesicle glycoprotein 2A; D: Nuclear cap binding protein subunit 1; E: Carbamoyl phosphate synthetase 1; F: Cytochrome c oxidase subunit 4 isoform 1; G: ATP synthase beta subunit precursor 1; H: Doublecortin like kinase 3. [a]*P* < 0.01 *vs* normal group; [b]*P* < 0.01 *vs* dextran sulfate sodium-induced ulcerative colitis model group. N: Normal group; M: Dextran sulfate sodium-induced ulcerative colitis model group; HM: Herb-partitioned moxibustion group; EA: Electroacupuncture group; Sv2a: Synaptic vesicle glycoprotein 2A; Ncbp1: Nuclear cap binding protein subunit 1; Cps1: Carbamoyl phosphate synthetase 1; Cox4i1: Cytochrome c oxidase subunit 4 isoform 1; Atp5f1: ATP synthase beta subunit precursor; Dclk3: Doublecortin like kinase 3.

of proteomics, we selected 6 DEPs that could be reversed by HM and EA for verification. We found that both HM and EA decreased the expression of Sv2a, Ncbp1, Cps1, Cox4i1, Atp5f1 and increased the expression of Dclk3, which were consistent with the iTRAQ results, confirming the reliability of the iTRAQ results. Cox4i1 is the main subunit of cytochrome c oxidase, a key enzyme in energy metabolism, and plays an important role in mitochondrial oxidative phosphorylation. Defects in oxidative phosphorylation leads to a decrease in cellular ATP production. Studies have reported that the activity of mitochondrial respiratory chain complexes in UC patients is reduced, and mucosal ATP is absent[50, 51]. Atp5f1 is a nuclear gene responsible for encoding the F0 subunit of ATP synthase, which is closely related to energy metabolism. Studies have found that the high expression of Cps1 plays an important role in the formation stage from UC to colitis associated cancer[52]. The intestinal mucosa of UC patients has been under chronic stress for a long time. The dynamic balance between oxidation and antioxidant defense mechanisms in the body is broken, causing mitochondrial damage, weakened oxidative phosphorylation, and reduced energy supply, which in turn causes cell apoptosis and colonic mucosal barrier dysfunction. The above results showed that HM and EA play a therapeutic effect on UC for mitochondrial function and energy metabolism. However, the role of Sv2a, Ncbp1 and Dclk3 in UC or mitochondrial oxidative phosphorylation has not been reported yet, and further research is needed.

In summary, iTRAQ proteomics was used in this study to identify DEPs in the colon of DSS-induced UC rats, as well as proteins that could be regulated by EA and HM, and analysed the function of these DEPs. However, the specific mechanisms of these DEPs were still unclear. They may be involved in one or more regulatory pathways, thus participate in the pathogenesis of UC and the mechanism of EA and HM treatments. The underlying mechanisms may require further study through animal and cell experiments.

CONCLUSION

In conclusion, our study used proteomics to provide evidence that EA and HM might regulate immune-related pathways by regulating the expression of ATP5L, Atp5f1, Cox4i1 that associated with oxidative phosphorylation, thereby alleviating colonic inflammation of DSS-induced UC rats. Further investigations at the role of these proteins in UC will be helpful for revealing the pathogenesis and the mechanism of acupuncture and moxibustion on UC.

ARTICLE HIGHLIGHTS

Research background

Ulcerative colitis (UC) is a chronic, nonspecific intestinal inflammatory disease with unclear etiology. Our previous studies have confirmed that acupuncture and moxibustion is effective in treating UC, but the mechanisms of treatment is still not completely clarified. Proteomic technology has revealed a

variety of biological markers related to immunity and inflammation in UC, which provide new insights and directions for the study of mechanism of acupuncture and moxibustion treatment of UC.

Research motivation

The mechanisms of UC and the therapeutic targets of acupuncture and moxibustion treatment are complicated, and whether acupuncture and moxibustion play a therapeutic role in UC by regulating proteome changes remains unclear.

Research objectives

The present study aims to investigate the underlying mechanism of electroacupuncture (EA) and moxibustion on UC rats by using isotope-labeled relative and absolute quantification (iTRAQ) proteomics technology.

Research methods

Male Sprague-Dawley rats were randomly divided into the normal (N) group, the DSS-induced UC model (M) group, the herb-partitioned moxibustion (HM) group, and the EA group. 3% DSS was used to establish the UC rat model except for the N group, and HM and EA at the Tianshu (bilateral) and Qihai acupoints were performed respectively. Haematoxylin and eosin staining was used for morphological evaluation of colon tissues. iTRAQ and liquid chromatography-tandem mass spectrometry were performed for proteome analysis of the colon tissues, followed by bioinformatics analysis and protein-protein interaction networks establishment of differentially expressed proteins (DEPs) between groups. Then western blot was used for verification of selected DEPs.

Research results

Our study revealed that HM and EA could regulate the expression of multiple proteins in colon of DSS-induced UC model rat. The DEPs were involved in various biological processes such as biological regulation, immune system progression and in multiple pathways including natural killer cell mediated cytotoxicity, intestinal immune network for immunoglobulin A production, and FcγR-mediated phagocytosis. Network analysis revealed that multiple pathways for the DEPs of each group were involved in protein-protein interactions. Subsequent verification of selected DEPs [synaptic vesicle glycoprotein 2A, nuclear cap binding protein subunit 1, carbamoyl phosphate synthetase 1, cytochrome c oxidase subunit 4 isoform 1 (Cox4i1), ATP synthase beta subunit precursor (Atp5F1), doublecortin like kinase 3] by western blot confirmed the reliability of the iTRAQ data.

Research conclusions

HM and EA might regulate immune-related pathways by regulating the expression of ATP5L, Atp5f1, Cox4i1 that associated with oxidative phosphorylation pathways, thereby alleviating colonic inflammation of DSS-induced UC rats.

Research perspectives

The present study revealed the possible molecular mechanisms of acupuncture and moxibustion treatment on UC, it may provide new light on clinical therapy of acupuncture and moxibustion treatment of UC.

ACKNOWLEDGEMENTS

The authors would like to acknowledge the Experimental Animal Center of Shanghai University of Traditional Chinese Medicine for providing the animals, acknowledge the Beijing Genomics Institute for technical services and support of proteomics testings.

FOOTNOTES

Author contributions: Wu LY, Huang Y and Qi Q conceived and designed this study; Zhong R, Liu YN, Ma Z and Zheng HD performed the animal experiments, acquired and analyzed the data; Qi Q wrote the main manuscript; Liu YN and Ma Z prepared the figures and tables; Lu Y gave guidance to the manuscript writing; Zhao C, Huang Y and Wu LY revised and improved the manuscript; and all authors reviewed and approved the final version of this manuscript.

Supported by the National Natural Science Foundation of China No. 81973955, 82004475 and 82174501; Shanghai Clinical Research Center for Acupuncture and Moxibustion No. 20MC1920500; Clinical Key Specialty Construction Foundation of Shanghai No. shslczdzk04701; Natural Science Foundation of Shanghai No. 21ZR1460200.

Institutional animal care and use committee statement: All animal experiments were performed according to the protocols approved by the Animal Ethics Committee of the Experimental Animal Center of Shanghai University of Traditional Chinese Medicine.

Conflict-of-interest statement: All the authors report no relevant conflicts of interest for this article.

Data sharing statement: No additional data are available.

ARRIVE guidelines statement: The authors have read the ARRIVE guidelines, and the manuscript has been prepared and revised according to the ARRIVE guidelines.

Country/Territory of origin: China

ORCID number: Qin Qi 0000-0002-0563-1560; Rui Zhong 0000-0002-5136-335X; Ya-Nan Liu 0000-0002-3290-9206; Chen Zhao 0000-0002-2872-6626; Yan Huang 0000-0002-5588-0274; Yuan Lu 0000-0001-7584-5727; Zhe Ma 0000-0003-0956-4438; Han-Dan Zheng 0000-0002-8640-9194; Lu-Yi Wu 0000-0001-8888-1698.

S-Editor: Wang JJ
L-Editor: A
P-Editor: Cai YX

REFERENCES

1 **Ungaro R**, Mehandru S, Allen PB, Peyrin-Biroulet L, Colombel JF. Ulcerative colitis. *Lancet* 2017; **389**: 1756-1770 [PMID: 27914657 DOI: 10.1016/S0140-6736(16)32126-2]
2 **Ng WK**, Wong SH, Ng SC. Changing epidemiological trends of inflammatory bowel disease in Asia. *Intest Res* 2016; **14**: 111-119 [PMID: 27175111 DOI: 10.5217/ir.2016.14.2.111]
3 **Wei SC**, Sollano J, Hui YT, Yu W, Santos Estrella PV, Llamado LJQ, Koram N. Epidemiology, burden of disease, and unmet needs in the treatment of ulcerative colitis in Asia. *Expert Rev Gastroenterol Hepatol* 2021; **15**: 275-289 [PMID: 33107344 DOI: 10.1080/17474124.2021.1840976]
4 **Du L**, Ha C. Epidemiology and Pathogenesis of Ulcerative Colitis. *Gastroenterol Clin North Am* 2020; **49**: 643-654 [PMID: 33121686 DOI: 10.1016/j.gtc.2020.07.005]
5 **Ji J**, Huang Y, Wang XF, Ma Z, Wu HG, Im H, Liu HR, Wu LY, Li J. Review of Clinical Studies of the Treatment of Ulcerative Colitis Using Acupuncture and Moxibustion. *Gastroenterol Res Pract* 2016; **2016**: 9248589 [PMID: 27885326 DOI: 10.1155/2016/9248589]
6 **Yang L**, Zhao JM, Guan X, Wang XM, Zhao C, Liu HR, Wu LY, Ji J, Cheng F, Liu XR, Wu HG. Observation on the effects of different partitioned moxibustion in treating ulcerative colitis. *J Acupunct Tuina Sci* 2016; **14**: 231-241 [DOI: 10.1007/s11726-016-0931-5]
7 **Lin YY**, Zhao JM, Ji YJ, Ma Z, Zheng HD, Huang Y, Cui YH, Lu Y, Wu HG. Typical ulcerative colitis treated by herbs-partitioned moxibustion: A case report. *World J Clin Cases* 2020; **8**: 1515-1524 [PMID: 32368545 DOI: 10.12998/wjcc.v8.i8.1515]
8 **Li YH**, Sun W, Zhou BJ, Rosenstein A, Zhao J, Wang J, Bian ZX. iTRAQ-based pharmacoproteomics reveals potential targets of berberine, a promising therapy for ulcerative colitis. *Eur J Pharmacol* 2019; **850**: 167-179 [PMID: 30771347 DOI: 10.1016/j.ejphar.2019.02.021]
9 **Schniers A**, Goll R, Pasing Y, Sørbye SW, Florholmen J, Hansen T. Ulcerative colitis: functional analysis of the in-depth proteome. *Clin Proteomics* 2019; **16**: 4 [PMID: 30718987 DOI: 10.1186/s12014-019-9224-6]
10 **Pisani LF**, Moriggi M, Gelfi C, Vecchi M, Pastorelli L. Proteomic insights on the metabolism in inflammatory bowel disease. *World J Gastroenterol* 2020; **26**: 696-705 [PMID: 32116417 DOI: 10.3748/wjg.v26.i7.696]
11 **Liu W**, Chen Y, Golan MA, Annunziata ML, Du J, Dougherty U, Kong J, Musch M, Huang Y, Pekow J, Zheng C, Bissonnette M, Hanauer SB, Li YC. Intestinal epithelial vitamin D receptor signaling inhibits experimental colitis. *J Clin Invest* 2013; **123**: 3983-3996 [PMID: 23945234 DOI: 10.1172/JCI65842]
12 **Yu SG**. Experimental Acupuncture. Beijing: People's medical publishing house, 2012
13 **Huang Y**, Ma Z, Cui YH, Dong HS, Zhao JM, Dou CZ, Liu HR, Li J, Wu HG. Effects of Herb-Partitioned Moxibustion on the miRNA Expression Profiles in Colon from Rats with DSS-Induced Ulcerative Colitis. *Evid Based Complement Alternat Med* 2017; **2017**: 1767301 [PMID: 28246536 DOI: 10.1155/2017/1767301]
14 **Li H**, Li KS, Wu LY, Zhou ZG, Huang RJ, Wu HG, Liu YN, Huang Y, Ma XP, Liu HR, Lu Y. Study on the Regulatory Effects of Acupuncture on Vitamin D Receptor and p53 Signal Pathway in Ulcerative Colitis Rats. *World Chinese Med* 2020; **15**: 2259-63+70 [DOI: 10.3969/j.issn.1673-7202.2020.15.012]
15 **Wang L**, Xie H, Xu L, Liao Q, Wan S, Yu Z, Lin D, Zhang B, Lv Z, Wu Z, Sun X. rSj16 Protects against DSS-Induced

Colitis by Inhibiting the PPAR-α Signaling Pathway. *Theranostics* 2017; **7**: 3446-3460 [PMID: 28912887 DOI: 10.7150/thno.20359]

16 **Lu Y**, Ding G, Zheng H, Lü T, Ma Z, Wu H, Weng Z, Zhang F, Wu L, Liu H, Xu M, Feng H. Effect of herb-partitioned moxibustion on dopamine levels and dopamine receptor 1 expression in the colon and central nervous system in rats with Crohn's disease. *J Tradit Chin Med* 2019; **39**: 356-363 [PMID: 32186008]

17 **Li N**, Xu Z, Zhai L, Li Y, Fan F, Zheng J, Xu P, He F. Rapid development of proteomics in China: from the perspective of the Human Liver Proteome Project and technology development. *Sci China Life Sci* 2014; **57**: 1162-1171 [PMID: 25119674 DOI: 10.1007/s11427-014-4714-2]

18 **Lees T**, Nassif N, Simpson A, Shad-Kaneez F, Martiniello-Wilks R, Lin Y, Jones A, Qu X, Lal S. Recent advances in molecular biomarkers for diabetes mellitus: a systematic review. *Biomarkers* 2017; **22**: 604-613 [PMID: 28074664 DOI: 10.1080/1354750X.2017.1279216]

19 **Zhang YF**. Differential proteomics analysis of tissues from ulcerative colitis patients and the establishment of acute damaged models with ulcerative colitis. Medical College of the Chinese People's Liberation Army, 2012

20 **Jin L**, Li L, Hu C, Paez-Cortez J, Bi Y, Macoritto M, Cao S, Tian Y. Integrative Analysis of Transcriptomic and Proteomic Profiling in Inflammatory Bowel Disease Colon Biopsies. *Inflamm Bowel Dis* 2019; **25**: 1906-1918 [PMID: 31173627 DOI: 10.1093/ibd/izz111]

21 **Ahmad A**, Ansari MM, Mishra RK, Kumar A, Vyawahare A, Verma RK, Raza SS, Khan R. Enteric-coated gelatin nanoparticles mediated oral delivery of 5-aminosalicylic acid alleviates severity of DSS-induced ulcerative colitis. *Mater Sci Eng C Mater Biol Appl* 2021; **119**: 111582 [PMID: 33321628 DOI: 10.1016/j.msec.2020.111582]

22 **Mishra RK**, Ahmad A, Kumar A, Vyawahare A, Raza SS, Khan R. Lipid-based nanocarrier-mediated targeted delivery of celecoxib attenuate severity of ulcerative colitis. *Mater Sci Eng C Mater Biol Appl* 2020; **116**: 111103 [PMID: 32806257 DOI: 10.1016/j.msec.2020.111103]

23 **Lo Sasso G**, Phillips BW, Sewer A, Battey JND, Kondylis A, Talikka M, Titz B, Guedj E, Peric D, Bornand D, Dulize R, Merg C, Corciulo M, Ouadi S, Yanuar R, Tung CK, Ivanov NV, Peitsch MC, Hoeng J. The reduction of DSS-induced colitis severity in mice exposed to cigarette smoke is linked to immune modulation and microbial shifts. *Sci Rep* 2020; **10**: 3829 [PMID: 32123204 DOI: 10.1038/s41598-020-60175-3]

24 **Simovic Markovic B**, Nikolic A, Gazdic M, Bojic S, Vucicevic L, Kosic M, Mitrovic S, Milosavljevic M, Besra G, Trajkovic V, Arsenijevic N, Lukic ML, Volarevic V. Galectin-3 Plays an Important Pro-inflammatory Role in the Induction Phase of Acute Colitis by Promoting Activation of NLRP3 Inflammasome and Production of IL-1β in Macrophages. *J Crohns Colitis* 2016; **10**: 593-606 [PMID: 26786981 DOI: 10.1093/ecco-jcc/jjw013]

25 **Papa Gobbi R**, De Francesco N, Bondar C, Muglia C, Chirdo F, Rumbo M, Rocca A, Toscano MA, Sambuelli A, Rabinovich GA, Docena GH. A galectin-specific signature in the gut delineates Crohn's disease and ulcerative colitis from other human inflammatory intestinal disorders. *Biofactors* 2016; **42**: 93-105 [PMID: 26891020 DOI: 10.1002/biof.1252]

26 **Simard JC**, Cesaro A, Chapeton-Montes J, Tardif M, Antoine F, Girard D, Tessier PA. S100A8 and S100A9 induce cytokine expression and regulate the NLRP3 inflammasome *via* ROS-dependent activation of NF-κB(1.). *PLoS One* 2013; **8**: e72138 [PMID: 23977231 DOI: 10.1371/journal.pone.0072138]

27 **Sekiya S**, Murata M, Arai S, Murayama H, Kawasaki A, Ashida N, Okada K, Ikemoto M. Enzyme-linked immunosorbent assay for S100A9 in the stool of rats with dextran sulfate sodium-induced colitis. *J Immunol Methods* 2016; **439**: 44-49 [PMID: 27693389 DOI: 10.1016/j.jim.2016.09.009]

28 **Steinbrecher KA**, Harmel-Laws E, Garin-Laflam MP, Mann EA, Bezerra LD, Hogan SP, Cohen MB. Murine guanylate cyclase C regulates colonic injury and inflammation. *J Immunol* 2011; **186**: 7205-7214 [PMID: 21555532 DOI: 10.4049/jimmunol.1002469]

29 **Brenna Ø**, Furnes MW, Munkvold B, Kidd M, Sandvik AK, Gustafsson BI. Cellular localization of guanylin and uroguanylin mRNAs in human and rat duodenal and colonic mucosa. *Cell Tissue Res* 2016; **365**: 331-341 [PMID: 27044258 DOI: 10.1007/s00441-016-2393-y]

30 **Brentnall TA**, Pan S, Bronner MP, Crispin DA, Mirzaei H, Cooke K, Tamura Y, Nikolskaya T, Jebailey L, Goodlett DR, McIntosh M, Aebersold R, Rabinovitch PS, Chen R. Proteins That Underlie Neoplastic Progression of Ulcerative Colitis. *Proteomics Clin Appl* 2009; **3**: 1326 [PMID: 20098637 DOI: 10.1002/prca.200900061]

31 **Wang D**, Zhang Y, Yang S, Zhao D, Wang M. A polysaccharide from cultured mycelium of Hericium erinaceus relieves ulcerative colitis by counteracting oxidative stress and improving mitochondrial function. *Int J Biol Macromol* 2019; **125**: 572-579 [PMID: 30543884 DOI: 10.1016/j.ijbiomac.2018.12.092]

32 **Nyström EEL**, Arike L, Ehrencrona E, Hansson GC, Johansson MEV. Calcium-activated chloride channel regulator 1 (CLCA1) forms non-covalent oligomers in colonic mucus and has mucin 2-processing properties. *J Biol Chem* 2019; **294**: 17075-17089 [PMID: 31570526 DOI: 10.1074/jbc.RA119.009940]

33 **Nyström EEL**, Birchenough GMH, van der Post S, Arike L, Gruber AD, Hansson GC, Johansson MEV. Calcium-activated Chloride Channel Regulator 1 (CLCA1) Controls Mucus Expansion in Colon by Proteolytic Activity. *EBioMedicine* 2018; **33**: 134-143 [PMID: 29885864 DOI: 10.1016/j.ebiom.2018.05.031]

34 **Erickson NA**, Mundhenk L, Giovannini S, Glauben R, Heimesaat MM, Gruber AD. Role of goblet cell protein CLCA1 in murine DSS colitis. *J Inflamm (Lond)* 2016; **13**: 5 [PMID: 26855614 DOI: 10.1186/s12950-016-0113-8]

35 **Li X**, Hu W, Zhou J, Huang Y, Peng J, Yuan Y, Yu J, Zheng S. CLCA1 suppresses colorectal cancer aggressiveness *via* inhibition of the Wnt/beta-catenin signaling pathway. *Cell Commun Signal* 2017; **15**: 38 [PMID: 28974231 DOI: 10.1186/s12964-017-0192-z]

36 **Bian Q**, Chen J, Qiu W, Peng C, Song M, Sun X, Liu Y, Ding F, Zhang L. Four targeted genes for predicting the prognosis of colorectal cancer: A bioinformatics analysis case. *Oncol Lett* 2019; **18**: 5043-5054 [PMID: 31612015 DOI: 10.3892/ol.2019.10866]

37 **Hu D**, Ansari D, Bauden M, Zhou Q, Andersson R. The Emerging Role of Calcium-activated Chloride Channel Regulator 1 in Cancer. *Anticancer Res* 2019; **39**: 1661-1666 [PMID: 30952704 DOI: 10.21873/anticanres.13271]

38 **Lu PD**, Zhao YH. Targeting NF-κB pathway for treating ulcerative colitis: comprehensive regulatory characteristics of Chinese medicines. *Chin Med* 2020; **15**: 15 [PMID: 32063999 DOI: 10.1186/s13020-020-0296-z]

39 **Wang Y**, Tang Q, Duan P, Yang L. Curcumin as a therapeutic agent for blocking NF-κB activation in ulcerative colitis. *Immunopharmacol Immunotoxicol* 2018; **40**: 476-482 [PMID: 30111198 DOI: 10.1080/08923973.2018.1469145]

40 **Huang XL**, Xu J, Zhang XH, Qiu BY, Peng L, Zhang M, Gan HT. PI3K/Akt signaling pathway is involved in the pathogenesis of ulcerative colitis. *Inflamm Res* 2011; **60**: 727-734 [PMID: 21442372 DOI: 10.1007/s00011-011-0325-6]

41 **Wei J**, Feng J. Signaling pathways associated with inflammatory bowel disease. *Recent Pat Inflamm Allergy Drug Discov* 2010; **4**: 105-117 [PMID: 20001899 DOI: 10.2174/187221310791163071]

42 **Atreya I**, Atreya R, Neurath MF. NF-kappaB in inflammatory bowel disease. *J Intern Med* 2008; **263**: 591-596 [PMID: 18479258 DOI: 10.1111/j.1365-2796.2008.01953.x]

43 **Castro-Dopico T**, Clatworthy MR. IgG and Fcγ Receptors in Intestinal Immunity and Inflammation. *Front Immunol* 2019; **10**: 805 [PMID: 31031776 DOI: 10.3389/fimmu.2019.00805]

44 **Castro-Dopico T**, Dennison TW, Ferdinand JR, Mathews RJ, Fleming A, Clift D, Stewart BJ, Jing C, Strongili K, Labzin LI, Monk EJM, Saeb-Parsy K, Bryant CE, Clare S, Parkes M, Clatworthy MR. Anti-commensal IgG Drives Intestinal Inflammation and Type 17 Immunity in Ulcerative Colitis. *Immunity* 2019; **50**: 1099-1114.e10 [PMID: 30876876 DOI: 10.1016/j.immuni.2019.02.006]

45 **Xie D**, Zhang Y, Qu H. Crucial genes of inflammatory bowel diseases explored by gene expression profiling analysis. *Scand J Gastroenterol* 2018; **53**: 685-691 [PMID: 29909694 DOI: 10.1080/00365521.2018.1461923]

46 **Shi W**, Zou R, Yang M, Mai L, Ren J, Wen J, Liu Z, Lai R. Analysis of Genes Involved in Ulcerative Colitis Activity and Tumorigenesis Through Systematic Mining of Gene Co-expression Networks. *Front Physiol* 2019; **10**: 662 [PMID: 31214045 DOI: 10.3389/fphys.2019.00662]

47 **Wang F**, Song Z, Chen J, Wu Q, Zhou X, Ni X, Dai J. The immunosuppressive functions of two novel tick serpins, HlSerpin-a and HlSerpin-b, from Haemaphysalis longicornis. *Immunology* 2020; **159**: 109-120 [PMID: 31606893 DOI: 10.1111/imm.13130]

48 **Lucas A**, Yaron JR, Zhang L, Ambadapadi S. Overview of Serpins and Their Roles in Biological Systems. *Methods Mol Biol* 2018; **1826**: 1-7 [PMID: 30194590 DOI: 10.1007/978-1-4939-8645-3_1]

49 **Mkaouar H**, Mariaule V, Rhimi S, Hernandez J, Kriaa A, Jablaoui A, Akermi N, Maguin E, Lesner A, Korkmaz B, Rhimi M. Gut Serpinome: Emerging Evidence in IBD. *Int J Mol Sci* 2021; **22** [PMID: 34200095 DOI: 10.3390/ijms22116088]

50 **Sifroni KG**, Damiani CR, Stoffel C, Cardoso MR, Ferreira GK, Jeremias IC, Rezin GT, Scaini G, Schuck PF, Dal-Pizzol F, Streck EL. Mitochondrial respiratory chain in the colonic mucosal of patients with ulcerative colitis. *Mol Cell Biochem* 2010; **342**: 111-115 [PMID: 20440543 DOI: 10.1007/s11010-010-0474-x]

51 **Santhanam S**, Rajamanickam S, Motamarry A, Ramakrishna BS, Amirtharaj JG, Ramachandran A, Pulimood A, Venkatraman A. Mitochondrial electron transport chain complex dysfunction in the colonic mucosa in ulcerative colitis. *Inflamm Bowel Dis* 2012; **18**: 2158-2168 [PMID: 22374887 DOI: 10.1002/ibd.22926]

52 **Lee YY**, Li CF, Lin CY, Lee SW, Sheu MJ, Lin LC, Chen TJ, Wu TF, Hsing CH. Overexpression of CPS1 is an independent negative prognosticator in rectal cancers receiving concurrent chemoradiotherapy. *Tumour Biol* 2014; **35**: 11097-11105 [PMID: 25099619 DOI: 10.1007/s13277-014-2425-8]

Published by **Baishideng Publishing Group Inc**
7041 Koll Center Parkway, Suite 160, Pleasanton, CA 94566, USA
Telephone: +1-925-3991568
E-mail: bpgoffice@wjgnet.com
Help Desk: https://www.f6publishing.com/helpdesk
https://www.wjgnet.com